April 2010

SAE Baja Gearless Differential 2009-2010

Brandon Marcus Pare
Worcester Polytechnic Institute

Cynthia C. Clark
Worcester Polytechnic Institute

Justin K. Goodwin
Worcester Polytechnic Institute

Kemal F. Moise
Worcester Polytechnic Institute

Konstantinos Dionysios Filiotis
Worcester Polytechnic Institute

See next page for additional authors

Author
Brandon Marcus Pare, Cynthia C. Clark, Justin K. Goodwin, Kemal F. Moise, Konstantinos Dionysios Filiotis, and Patrick J. Fraser

SAE Baja Gearless Differential 2009-2010

A Major Qualifying Project Report
Submitted to the Faculty of
WORCESTER POLYTECHNIC INSTITUTE
In partial fulfillment of the requirements for the
Degree of Bachelor of Science
By:

Konstantinos Filiotis

Patrick Fraser

Justin Goodwin

Kemal Moise

Brandon Pare

Cynthia Weiler

Date: April 23, 2010

Eben C Cobb, Advisor

Torbjorn Bergstrom, Advisor

Contents

List of Figures v

List of Tables v

Authorship vi

Abstract vi

Introduction 1

Background Research 3

Goal Statement 9

Task Specifications 9

Design Description 11

Torque Analysis 13

Kinematic Analysis 14

Sprocket Design 17

Sprocket Teeth Geometry Equations 18

Flange Thickness and Tooth Section Profile 21

Sizing the Hub 22

Hub-Carrier Finite Element Analysis 22

Preparation 23

Results 24

Manufacturing Process and Results 26

Hubs 26

Carrier 27

Cams 28

Pilot Pin 29

Bushings 29

Sliding Ball Bearings 30

Internal and External Frame mounts 30

Frame Alterations 31

Recommendations for Machining 32

Conclusions and Recommendations 32

Bibliography / Vendor Information 37

Appendix A: Bill of Materials and Chassis Assembly 39

Appendix B: Differential Assembly 41

Appendix C: Hub (No Sprocket) 44

Appendix D: Cam Bushing 45

Appendix E: Cam (Left Hand) 46

Appendix F: Pilot Bushing 48

Appendix G: Carrier 49

Appendix H: Ball Point Support 50

Appendix I: Inner (Small) Ball 51

Appendix J: Outer (Large) Ball 52

Appendix K: V-Cut Ball Support 53

Appendix L: Pilot Pin 54

Appendix M: Cam (Right Hand) 55

Appendix N: Hub (With Sprocket) 57

Appendix O: Internal Bearing Mount 60

Appendix P: External Bearing Mount 61

Appendix Q: Bearing Housing Assembly 62

Appendix R: American National Standard Roller Chain Sprocket Flange Thickness and Tooth Section Profile Dimension 63

Appendix S: Typical Proportions of Roller Chain Sprockets 64

Appendix T: ANSI Sprocket Tooth Form For Roller Chain 65

Appendix U: Fastening MathCAD and Wrench Torque Table 66

Appendix V : Sprocket Dimension MathCAD 67

Appendix W: Stock Dimensions 69

Appendix X: Free Body Diagrams 71

List of Figures

Figure 1: SAE Baja Car 2008-2009 1

Figure 2: Labeled Cross Sectional View of Differential Assembly 11

Figure 3: Sprocket Diameter 21

Figure 4: FEA Discrete Von Mises Plot 24

Figure 5: Stress Intensity Discrete Plot 25

Figure 6: Exploded View of Differential Assembly 26

Figure 7: Machined Side of Carrier 28

Figure 8: Machined Cam 28

Figure 9: Pilot Pin 29

Figure 10: Machined Cam Bushing 29

Figure 11: Altered Ball Bearings (Tsiriggakis,2003) 30

Figure 12: Section of Frame to be Removed 31

Figure 13: Carrier, Cam, and Cam Bushing 32

Figure 14: Machinery's Handbook (pg 2459) 63

Figure 15: Machinery's Handbook (pg 2460) 64

Figure 16: Machinery's Handbook (pg 2468) 65

Figure 17: Machinery's Handbook (pg 1429) 66

List of Tables

Table 1: Comparison Table for Various Types of Differentials 7

Table 2: #428 Motorcycle Chain Geometry 18

Authorship

CAD models and drawings were done primarily by Pat Fraser. The rest of this report was created through the equal contributions of all group members: Konstantinos Filiotis, Pat Fraser, Justin Goodwin, Kemal Moise, Brandon Pare, and Cynthia Weiler.

Abstract

Most wheeled vehicles around the world are using some form of differential to improve both performance and safety. Use of a solid axle does not allow the two wheels to rotate at different speeds, which poses serious handling issues while turning. When cornering, the vehicles outside wheels travel further in the same time period as the inside; and if an outside wheel is not allowed to travel faster, wheel slippage is unavoidable. A solid axle however, is beneficial because it provides power to both wheels at all times. This was a distinct concern with the ‘09 model of the SAE Baja vehicle. The focus of the project was to provide a solution to this issue. A gearless differential was selected as a solution to provide differentiation between the wheels while limiting slip during acceleration giving some of the benefits of a solid axle.

Introduction

This report documents the design of a gearless differential for use within the SAE Baja competition vehicle. The previous competition vehicle had troubles with cornering, as wheel slippage was a factor in the overall performance of the vehicle. In particular, the previous method for power transmission to the wheels was a solid axle setup without any differential. So design of a differential for use within the car was considered to combat these effects and increase the overall performance of the vehicle.

Figure 1: SAE Baja Car 2008-2009

Generally, for effective cornering the outside wheel requires that it travel further and spin faster than the inside wheel. A simple solid axle setup does not allow for these dynamics. Almost every automobile uses a differential to allow the inner and outer wheels to spin at different speeds while still transferring the same power uniformly. This is universally accepted as an ideal method and employed in more than just automobile drive trains. The internal design of the differential plays an important role in the mechanics of the device.

Numerous differential designs are available each of which providing a different structure within the differential. Including, but not limited to Torsen differentials, open differentials,

locking differentials, and limited slip differentials. Internally there are multiple variations as well, including geared differentials which transmit power through the mesh of the gears, as well as gearless differentials which use balls or friction plates to transmit power through applied forces over surface areas.

Selection of a gearless differential for this design was optimal as the inability to cut gear teeth was a considerable design factor. Current methods available to manufacture the differential facilitate the choice of a gearless differential without having to outsource manufacturing and increase costs. Thus the choice of a ball differential was settled upon. More specifically the design mimics closely the parameters of a Tsirigakkis Differential which will be elaborated on in the design description section of this report.

Background Research

Since the beginning of time, the differential has been used in numerous types of machinery. The differential's ability to combine multiple inputs and outputs into one device is what makes it so versatile, as well as its compact design. This versatility has carried over through time and eventually the differential found its way into automobiles and powered vehicles. As technology progressed so did the need for a device that would allow a vehicle to corner more efficiently.

Before the differential, most methods for transmission of power from the engine to the wheels and axle were simple solid axles with a single fixed input on a shaft connecting the two wheels. This setup is what currently resides in the current SAE Baja vehicle, and it has been shown in previous competitions that the vehicle corners quite poorly because of its straight axle setup. The issue arose that when cornering, the inside and outside wheels need to rotate at different speeds because they cover different distances. With a solid axle setup, this is impossible as both wheels are forced to rotate at the same speed, or what's known as wheel slipping. This effect of traction loss caused unnecessary wear on the wheel where traction is least available. Regardless of road or surface condition, the solid axle transmits the same torque to both wheels. Essentially one wheel slides through the corner rather than rotating and causing the vehicle to under steer while cornering. Under steer is when a vehicle is unable to follow the arc of the corner, and it starts to veer outwardly away from the arc. Reducing the applied torque allows the outer wheel to regain traction partially. This allows the vehicle to regain some cornering ability but ultimately the outer wheel still continues to slide. Tire sliding causes uneven wear of the

tires, which causes traction problems, which gets worse the more a tire is worn. To combat this ill-effect of wheel slippage, numerous different designs of differentials have arisen to provide different handling characteristics for differing traction situations.

There are numerous differential designs available commercially. Each type offers different traction characteristics as well as internal mechanics. Generally, there is considered limited slip (LSD), locking differential, or an open differential. A Limited slip differential or LSD allows for a more controlled differentiation of wheel speed. A threshold is set by the mechanics of the differential that allow a certain amount of free wheel spinning before the LSD transfers a portion of the total available torque to the wheel with the most grip.

Two main types of LSD exist, torque sensitive (geared or clutch-based) and speed sensitive (viscous/pump and clutch pack) (Differential, 2010). Each type provides different traction-controlling methods but generally torque sensitive LSD's are used in high performance applications for their ability to transfer torque to the wheel with the most traction. Torsen differentials fall under the category of torque sensing LSD's. Speed sensitive LSD's work under the properties of high viscosity silicon oils and fluids where the fluid heats up within the LSD and pushes perforated discs against each other causing the "locking" action desired.

Locking differentials provide an alternative to traction loss by locking both wheels together while under power in a straight line, and "unlock" the outer wheel if externally made to rotate faster while cornering. Although seemingly ideal, the unlocking process only occurs when there is minimal or no power applied by the driveshaft. The two operations of a locking

differential are opposite in nature and often alternates between one wheel and two wheel drive while cornering under power making for difficult to control handling (Differential, 2010). Locking differentials also come in a variety of controllable locking mechanisms which is driver selectable. The differential is essentially an open differential with a mechanism to lock the two shafts together when desired. Methods include compressed air, mechanical cable, electric actuator or hydraulic fluid to activate the locking mechanism (Differential, 2010).

An open differential is a basic design, and for everyday vehicles is an optimal design. Torque generated by the drive shaft is split between the two halves of the differential and in cases where one wheel has less traction, torque is transferred to that wheel which is considered more “free”. This is less than ideal in off-road conditions, where traction is minimal and wheel spin occurs during cornering causing unnecessary over steer. Straight line propulsion is affected as well, for low traction conditions. One wheel becomes the single driving wheel to move the vehicle forward while the other wheel is free to rotate without power. Open differentials are ideal for paved surfaces where traction is ideal.

Internally differentials vary as has been shown. But an alternative to geared differentials exists in the form of a ball differential. A ball differential relies on thrust washers that push against the balls or ball bearings inside the gear by Belleville washers. The adjusting collar, allows for adjustments in the amount of slip allowed by the differential. The thrust bearing on the opposite side of the gear is used to stop the differential from loosening the retaining screw holding the output cups, used to attach the differential to the axle, onto the differential. As the screw is tightened, it pushes the Belleville and thrust washers onto the gear. This creates the

contact friction forces between the washers and ball bearings inside the gear. Friction is often aided by silicone grease. As the washer on the opposite side of the gear rotates, the rotation of the balls causes the other washer to rotate in the opposite direction. Differentiation occurs because the thrust washers rotate with the ball bearings. The retaining screw is designed such that the differential can be easily adjusted in comparison to geared differentials (Bavonics, 2005). An example of a simpler ball differential is the Tsirigakkis differential that utilizes ball bearings that ride on sinusoidal face cams connected to output shafts. The offset face cams allow for differentiation in wheel speed while cornering by allowing the outer half of the differential to spin faster while the other half spins slower much like an open differential.

In researching the capabilities of the resources available, it was seen that a gearless differential was the optimal basis for a solution. With the inability to cut gear teeth, or the lack of available funding to outsource the production of gears, everything would have to be done in house with WPI's available manufacturing processes. Issues arise in the designing, machining, and assembly phases of the project. This is an unavoidable factor with producing a prototype. Taking into consideration input torque from the hydraulic drive train that was being developed for the vehicle could produce torque equivalent to that of a full size car, required that the differential be robust in initial sizing and design. Machining parts of the prototype are difficult as well. Depending on the knowledge and skill base of the machinist, machining certain parts of the prototype could potentially prove to be difficult if problems arise such as lack of proper tooling, incorrect material selection and tool selection, faulty machine code, or faulty machine tool operation. Proper planning and evaluation of machining methods must be taken to ensure smooth production. Even if all parts of the prototype are machined correctly, the assembly of the

prototype can prove to be problematic. These problems are prevalent in the process of creating a prototype no matter how polished the procedures are.

Different types of differentials were considered before choosing the limited slip gearless differential. “Table 1: Comparison Table for Various Types of Differentials” shows the different types and how we rated them against each other. The outcome of this comparison chart favors the Tsiriggakis differential and the solid axle set up with a negligible lean towards the sold axle. Despite the relative tie in the outcome of this comparison chart the Tsiriggakis differential was ultimately chosen for some of the reasons discussed but also for the sake of exploring the potential for improvement of the SAE Baja car.

Table 1: Comparison Table for Various Types of Differentials

See below table for brief description of each type of differential compared in this table.

Attribute		Cost	Off-road effectiveness	Reliability	In house machinability	Innovation		
Multiplier of Importance		2	5	3	4	1		**Total Scores adjusted by multiplier**
Type of Differential	Geared (locking)	1	5	3	2	3		**47**
	Geared (open)	4	1	6	3	2		**45**
	Torsen	2	6	2	1	5		**49**
	Cam	3	4	4	5	6		**64**
	Ball	5	2	1	4	4		**43**
	Solid axle	6	3	5	6	1		**67**

Geared (locking):

A conventional geared differential with a locking mechanism, either pneumatically or electronically engaged.

Geared (open):

A conventional geared differential with no resistance to differentiation and no locking mechanism.

Torsen:

A torque sensing limited slip differential that sense the loose of traction in one wheel, and applies torque to the wheel with more traction.

Cam:

The differential chosen for this project is a rare type of limited slip differential that uses cam tracks and ball bearings to distribute torque between the two wheels.

Ball:

A differential that uses the friction between ball bearings and a flat plat to transmit torque to the wheels. It is open and does not limit slip.

Solid axle (no differential):

In the absence of a differential the two wheels will always spin the same speed regardless of differences in traction.

Goal Statement

Create a gearless differential that interfaces with the current SAE Baja vehicle while improving the cornering ability of the vehicle, and includes locking or limited slip features to aid traction.

Task Specifications

- Design must be fitted into the vehicle in a manner that does not compromise structural integrity.
- Design must be compatible with other components of the drive train.
- Device must be entirely mechanical.
- Mechanism must withstand the forces exerted on it by the vehicle under both static and dynamic conditions.
- Mechanism must operate under the forces exerted on it by the vehicle under both static and dynamic conditions.
- The mechanism must be autonomous with the exception of any locking mechanism that may be attached.
- No assembly can violate any rules or regulations as defined by the official SAE Baja organization for the year 2010.
- All exposed parts must be resistant to corrosion
- The design and placement must not offset any pre-existing load balance of the vehicle.
- Design must be easily interchangeable with commercially available solutions (modular).

- Mechanism must apply appropriate torque distribution during all points of normal competitive operation.
- Design must be structurally robust while using the lightest materials possible.
- Must not fatigue under normal operation - 1 competition year.
- Manufacturing of the device must fit the capabilities of the WPI machine shop
- Design should utilize appropriate materials while minimizing cost
- Design must feature sealed internals
- Design must be properly lubricated to ensure longevity

Design Description

Before discussing the design of the Tsiriggakis differential, each part will be identified. From the center, outwards there is: (see Figure 2) the pilot pin, 2 pairs of bushings, 4 pairs of machined ball bearings (only 2 pairs visible in section view), 2 face cams on either side, and 2 hubs on the outer most of the differential, one with and one without a sprocket.

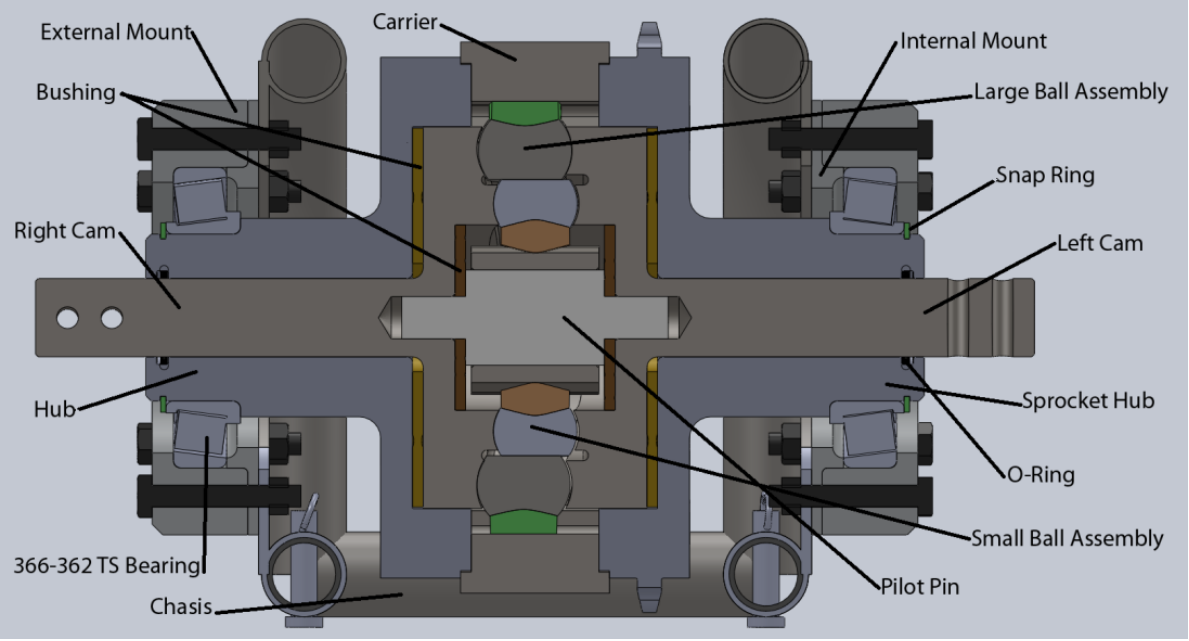

Figure 2: Labeled Cross Sectional View of Differential Assembly

This differential sits in the vehicle between the half shafts connecting to the rear wheels. It allows each shaft to rotate at different speeds. The drive sprocket on the right hub takes the input torque from the gear reduction/hydraulic drive train. The right hub is bolted to the central carrier and left hub. These 3 pieces rotate together at the same speed, around the cams, supported by bearings at both ends.

The carrier holds 8 custom ball bearings. Each ball is machined with a flat and an inward facing point. This allows the bearings to slide against each other and follow a point support on either end. The ball bearings are arranged in a cross pattern and sit between 2 concentric sinusoidal tracks on both the right and left cam face. The tracks are offset by 90 degrees such that all the balls are always in contact with each cam surface. The contact between the balls and the cam is what transfers torque from the sprocket on the hub to the cam faces and then to each half shaft, causing the wheels to rotate. The pilot pin and the bushings serve to circulate lubricant and take some of the axial loads from the half shafts.

However, because the half shafts are not connected to each other, each cam can slide past the bearings and rotate at different speeds. When either wheel needs to travel further, for example when going around a curve, or if either wheel meets with different resistance, the differential allows for power to be transmitted from the hydraulic drive train to both wheels while still letting them rotate at different speeds.

The Tsirgakkis differential is limited slip gearless differential. Limited slip simplifies the design since a locking mechanism no longer has to be implemented when the wheels do not need to differentiate. When both wheels are traveling the same distance or are met with equal resistance, the differential will act like a solid axel. Equal power will be transmitted to both wheels and they will turn at the same speed. However when either wheel begins to slip the differential will allow for each wheel to turn independently of the other. This will be useful while handling corners when the outside wheel has to turn a farther distance. It will also be useful

when one wheel is in the air and has no resistance at all. A traditional differential may have the raised wheel spinning and deliver no power to the wheel that actually has traction.

Having a gearless differential would considerably simplify the manufacturing process. Our goal was to be able to machine as many parts of whichever differential design was chosen in house, that is, in the Worcester Polytechnic Institute Machine Shops. This served 2 purposes. It would reduce the cost towards the group for parts that needed to be machined elsewhere. Complex parts, most notably gears, would need to be machined by private companies. We would have to pay for raw materials and labor at a price profitable for any external vendor. Also, Gears are difficult to machine and need to be machined and installed to very low tolerances to operate correctly, all of which would increase the price.

The other benefit is that it would reduce turnaround for new parts. It would be naïve to assume that all parts would be perfect the first time through. If any part breaks or is redesigned, a new part could be made as soon as new stock material gets in, typically in 2 days. Any new part from an external vendor would need to be requited, machined, delivered and could easily take 2 weeks or more to arrive.

Torque Analysis

To properly size the differential, basic calculations were performed in order to obtain an arbitrary applied torque from the hydraulic motor through the drive train. In the early stages of the overall design of the car, it was presumed that the drive train would have an overall gear

reduction of 9:1. This however was nearly impossible given the size of the differential. A sizable sprocket would have been needed, with at least 100+ teeth and a tremendously large diameter. Given the spatial constraints of the rear end, this was unacceptable. The design was simplified to two 3:1 reductions, the first being a planetary gear reduction attached to the hydraulic motor output, and then a chain and sprocket reduction with a gear ratio of 3:1. The hydraulic drive train team supplied a maximum torque output at a given maximum rpm; 60 N-m (or 44 lb-ft) at 3600rpm. To find the output torque from the planetary gear reduction, Prof. Norton's torque ratio for simple gear trains which states; $T_{out} = T_{in} \frac{\omega_{in}}{\omega_{out}}$ (Norton, 2008) was used. It states that the torque applied by the next gear is equal to the torque input from the first gear times the angular velocity ratio which is three. This is because the gear reduction ratio is 3:1 as the input gear spins three times, the output gear spins once. Performing this calculation once more gives the overall torque experienced by the differential, assuming that the drive train from the planetary sprocket to the differential has no slack. This number is 396 ft-lbs at 400rpm, granted this is at max rpm and merely just a theoretical number. In practicality the system will never experience these numbers due to the vehicle actually being put on the ground. This theoretical number allows for proper sizing and materials selection of the differential as well as allows for proper selection of the correct chain. (Norton, 2008)

Kinematic Analysis

The kinematic behavior of the various parts of the differential was to be analyzed for when the vehicle was both cornering and when it was moving in a straight line. The difficulty in doing this came due to the fact that there are no existing equations governing a gearless

differential such as this. A typical differential is classified as an epicyclical gear train with one input and two outputs that are coupled by friction (the road). For calculations, the gearless differential was considered to be an epicyclical gear train with the carrier as the arm, the sliding bearings as the planet gears, and the cam surfaces as the sun gears.

The issue with making calculations in this way is that the kinematic behavior of an epicyclical gear train with one input and two outputs cannot be predicted (Norton, 2008). In order for these equations to work, two inputs are needed. A method for calculating the angular velocities of the carrier and cams during complete differentiation was determined, however. During complete differentiation, one of the cams is fixed at zero velocity while the other rotates at maximum speed. By considering the non moving cam as an input with zero velocity, and the carrier as the other input, the velocity of the spinning cam can be determined.

The equations governing kinematics of an epicyclical gear train are largely dependent on the number of teeth on each gear in the train. The gearless differential has no gear teeth; however one can find the gear ratios between the components simply based on the diameter of the component. If gear ratios are known, the equivalent number of gear teeth for the gearless system can be found.

After finding the equivalent number of gear teeth of each component, the fundamental gear train value R was calculated. R is found using the equation:

$$R = \pm \frac{product\ of\ number\ of\ teeth\ on\ driver\ gears}{product\ of\ number\ of\ teeth\ on\ driven\ gears}$$

It was determined that the sprocket and rotating cam were driver gears, while the ball bearings and stationary cam were driven gears. Given this R was calculated as:

$$R = \pm\frac{N_1 N_6}{N_2 N_3 N_7}$$

Where N is the number of teeth on the given gear. The speed at the carrier was assumed to be 30 mph. Knowing the diameter of the sprocket the angular velocity of the carrier could be determined, which was found to be 162.462 radians per second and the angular velocity of the stationary cam was obviously 0 radians per second. Using the relationship:

$$\frac{N_1 N_6}{N_2 N_3 N_7} = \frac{\omega_L - \omega_a}{\omega_f - \omega_a}$$

Where N is the number of teeth on the given gear, ω_L is the angular velocity of the last gear (stationary shaft), ω_a is the angular velocity of the arm (carrier) and ω_f is the velocity of the spinning shaft. Solving for ω_f a value of -204.354 radians per second is attained. This is equivalent to about 26 miles per hour; the negative sign indicates that it spins the opposite direction of the other shaft.

At first thought one may think that the shaft should be rotating at the same 30 miles per hour as the carrier, however this is not true in this case. If this differential were completely open this would be true since an open differential will send 50% torque and 100% speed to the rotating side while sending 50% torque and 0% speed to the grounded side. With the limited slip design of the gearless differential however, there is always some speed transmitted to both sides to provide greater traction in all conditions accounting for the 4 mile per hour difference.

A simple visual analysis of the design gives a solution to the kinematics of the parts while the vehicle is moving in a straight line. Since when in a straight line the differential is essentially locked, the carrier and cams will be turning at the same speed.

Analysis was also done to determine the efficiency of the gearless differential. In order to solve for the efficiency the train ratio ρ must be found. This is done simply using the fundamental train value determined earlier. If the train value is greater than one than ρ =R, if the train value is less than 1 than ρ =1/R. Since the train value was .795, ρ was 1/R=1.258. Since ρ is greater than 1, the input shaft is shaft 1 and fixed shaft is shaft 2, this is a case 1 train. In a case 1 train efficiency is given as:

$$\eta = \frac{\rho E_0 - 1}{\rho - 1}$$

where E_0 is the basic efficiency of the gear set. Most all gear sets have an efficiency greater than .98, so the value of E_0 was assumed to be .98. A value of .902 was calculated meaning that the gearless differential is about 90% efficient (Norton, 2008). Detailed MathCAD solutions for all calculations can be found in the appendix.

Sprocket Design

The sprocket around the hub was designed based on three criteria; the type of chain to be used, the necessary gear ratio, and the number of chain strands used. The type of chain to be used is a #428 motorcycle chain, which has given geometry in Table 2 below.

Table 2: #428 Motorcycle Chain Geometry

Dimension	Value	Variable
Pitch	.500 in	P
Nominal Roller Diameter	.335 in	D_r

The necessary gear ratio between the hydraulic drive-train and the differential was set to be 3:1. The minimum number of teeth that the sprocket from the drive-train could have is 14 to ensure the number of teeth that would be engaged in the chain did not become too small. Using this value and the gear ratio, the number of teeth necessary around the sprocket must be 42 teeth, (N_t). A single strand configuration was used in the following calculations to dimension the sprocket.

Sprocket Teeth Geometry Equations

To accurately dimension the teeth around the sprocket, equations and values from Table 11: *ANSI Sprocket Tooth Form for Roller Chain* of ANSI/ASME B29.1M-1993 where used. Refer to Appendix T: ANSI Sprocket Tooth Form For Roller Chain for the general sprocket tooth geometry, a list of equations and calculations for the sprocket geometry. Many of the values to dimension the sprocket teeth have no true physical correlation and are only used to dimension the teeth. However, the described equations below go through the main variables used to design the sprocket teeth. All equations used are in English units. (Oberg, Jones and Horton)

The seating curve diameter (D_s) is the distance between the contact points of the chain roller and the sprocket teeth. This distance is dependent on the nominal roller diameter (D_r) and given by the equation below:

$$D_s = 1.005 * D_r + .003$$

The dimension *R* is the radius of the bottom of the sprocket tooth gap from the pitch diameter. This radius is based on the seating curve diameter (D_s) and given by the equation below:

$$R = \frac{D_s}{2}$$

The dimension *F* is the radius of the upper profile of the sprocket tooth. This dimension is dependent on the nominal roller diameter (D_r) and the number teeth on the sprocket (N_t). The equation for *F* is given below:

$$F = D_r * \left(0.8 * \cos\left(18° - \left(\frac{56°}{N_t}\right)\right) + 1.4 * \cos\left(17° - \left(\frac{64°}{N_t}\right)\right) - 1.3025\right) - .0015$$

The *H* dimension is the height of the sprocket tooth point from the seating curve diameter. This height is based on the radius of the upper tooth profile (*F*), the nominal roller diameter (D_r), and the pitch (*P*). The equation for the *H* dimension is given below:

$$H = \sqrt{F^2 - (1.4 * D_r - .5 * P)^2}$$

The *S* dimension is the linear distance between the center of the tooth gap and the tooth point. The *S* dimension is based on the pitch (*P*), the number of teeth (N_t), and the height of the

sprocket tooth point from the seating curve diameter (*H*). The following equation is used to find this distance:

$$S = .5 * P * \cos\left(\frac{180°}{N_t}\right) + H * \sin(\frac{180°}{N_t})$$

The value OD_f is called the flat tooth diameter and is the diameter over the tips of the sprocket teeth with flat tip tooth geometry. Flat tip tooth geometry was chosen to decrease the overall diameter of the sprocket. The equation for the flat tooth diameter is dependent on the pitch (*P*) and the number of teeth (N_t), and is given below:

$$OD_f = P * \left(0.6 + \frac{1}{\tan\left(\frac{180°}{N_t}\right)}\right)$$

The pitch diameter (*PD*) is the diameter of the pitch circle that passes through the centers of the link pins as the chain is wrapped on the sprocket. The pitch diameter equation is dependent on the pitch (*P*) and the number of teeth (N_t). The equation for pitch diameter is given below:

$$PD = \frac{P}{\sin\left(\frac{180°}{N_t}\right)}$$

The bottom diameter (*BD*) is the diameter of a circle tangent to the curve at the bottom of the tooth gap. The bottom diameter is dependent on the pitch diameter (*PD*) and the radius of the bottom of the sprocket tooth gap (*R*). Its equation is given below:

$$BD = PD - 0.2 * R$$

Figure 3 below shows the sprocket diameters as they relate to the sprocket geometry. (Oberg, Jones and Horton)

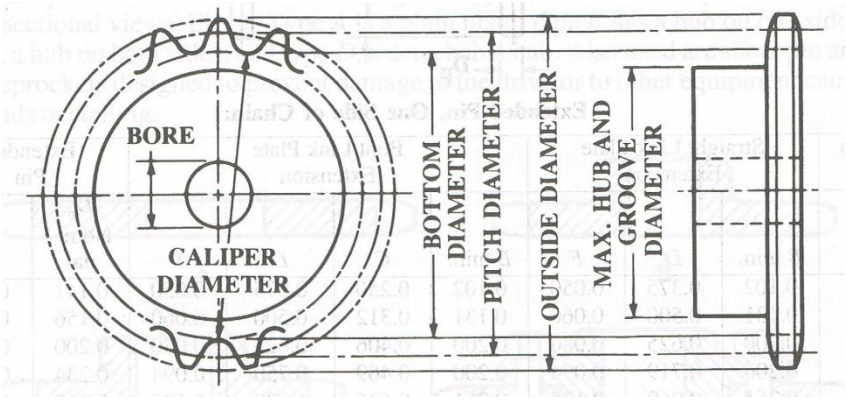

Figure 3: Sprocket Diameter

Flange Thickness and Tooth Section Profile

Once the sprocket tooth geometry has been established the next step for designing the sprocket is the flange thickness and the tooth section profile. These dimensions are given in Table 6: *American National Standard Roller Chain Sprocket Flange Thickness and Tooth Section Profile Dimension* of ANSI/ASME B29.1M-1993 (R1999) and shown in Appendix R: American National Standard Roller Chain Sprocket Flange Thickness and Tooth Section Profile Dimension. As stated above, the values found below are based on a single-strand configuration. Within the standard, the flange thickness is dependent on the width of the chain, given below:

$$W \approx \frac{5}{8}P$$

where W is the width of the chain and P is the pitch of the chain. The flange chamfer was chosen to follow Section "A" geometry as per the ANSI standard. The flange chamfer geometry is mainly dependent of the pitch of the chain. (Oberg, Jones and Horton)

Sizing the Hub

The final step for dimensioning the sprocket was to size the hub, the section of the sprocket that would not interact with chain. To size the hub the maximum hub diameter (*MHD*) was calculated based on Table 8: *Typical Properties of Roller Chain Sprockets* in Appendix S: Typical Proportions of Roller Chain Sprockets which is provided by the American Chain Association. The equation for calculating the maximum hub diameter is given below:

$$MHD = P * \left(\cot\left(\frac{180^\circ}{N_t}\right) - 1\right) - .030$$

where P is the pitch of the chain and N_t is the number of teeth on the sprocket. Following the MHD, the maximum hub radius (r_f) was then calculated. The maximum hub radius is the maximum allowable radius between the bottom of the sprocket teeth and the face of the hub. The equation for r_f is given below where P is the pitch of the chain. (Oberg, Jones and Horton)

$$r_f = 0.04 * P$$

Hub-Carrier Finite Element Analysis

To assist with the design of the differential, finite element analysis was performed on the structural and driving members of the differential. This analysis consists of three main components: the carrier, the sprocket hub, and the non-sprocket hub. The following sections describe the preparation and results of this analysis.

Preparation

The first step in the preparation was to assemble the components and assign materials to them. The carrier is made of AISI 1018 steel which has a yield strength (σ_y) = 370 MPa. Both hubs were assigned Al 6061-T6 and has a yield strength = 276 MPa. (Material Property Data, 2010)

Once the materials where assigned, bolt connections were mimicked at the 16 locations around the two hubs. The bolts used were standard .250-20 socket head cap screws made of zinc-plated alloy steel. Along with the positioning of the bolts, a preload was applied at each location. The preload was determine by the calculation of the wrench torque (T_{wrench}) in in-lbs and the bolt's friction coefficient (K) = 0.2 for zinc-plated bolts. The value for wrench torque is given by the equation below:

$$T_{wrenc\ h} = 10^{b+m*\log(d)}$$

where d is the diameter of the bolt and the values for b and m are constant values based on the fastener grade. The values for m and b are given in Appendix U: Fastening MathCAD and Wrench Torque Table. (Oberg, Jones and Horton)

The final step in the preparation of the model was to apply fixture and load surfaces to the assembly. A rotating fixture was applied to the bearing surfaces and for one-half of a rotation. A torque load was applied to the pitch diameter of the sprocket hub. The value for torque load was given from the predicted output torque of the hydraulic drive-train, T= 228 ft-lbs. Accounting for the 3:1 gear ratio the actual torque applied to the hub sprocket is around 684 ft-lbs.

Results

After applying a fine mesh to the model, Figure 4: FEA Discrete Von Mises PlotFigure 4 below displays the results of the finite element analysis in a discrete Von Mises plot.

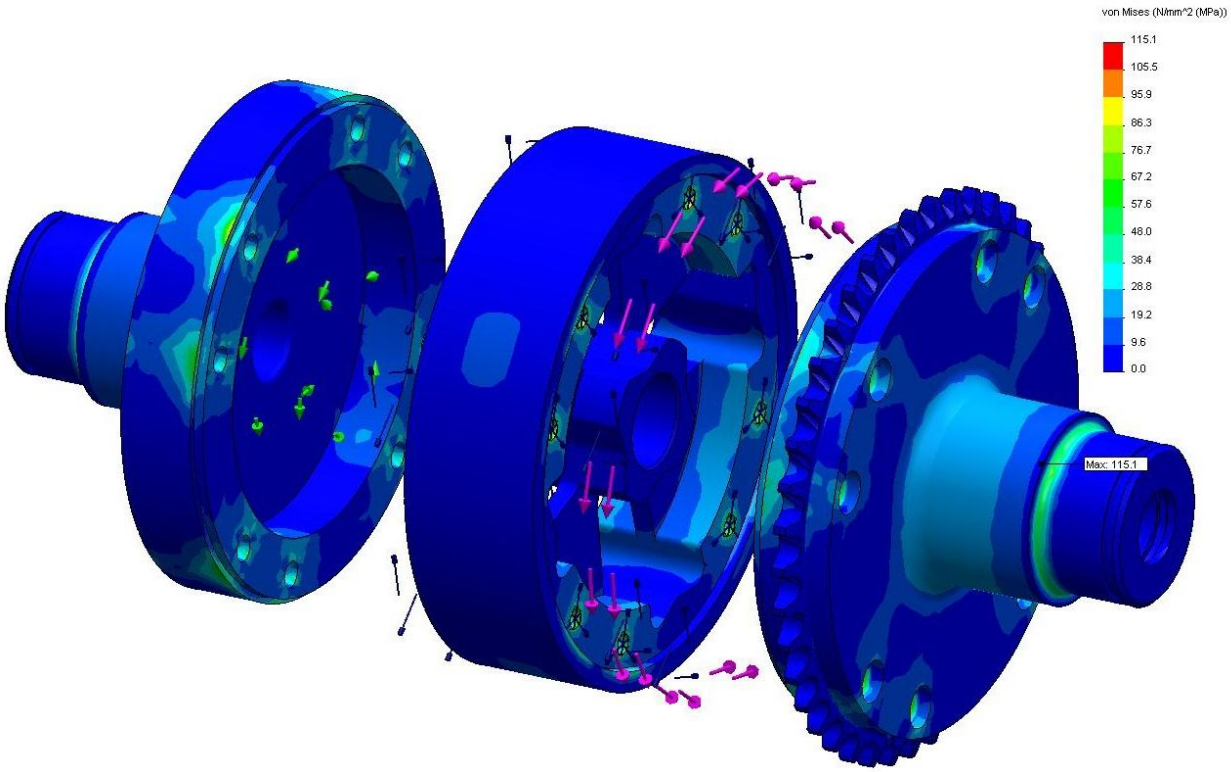

Figure 4: FEA Discrete Von Mises Plot

From the FEA, the maximum Von Mises stress is located at the bearing surface fillet on the hub and has a magnitude of 115.1 MPa. This value is well below the yield strength for the 6061 T6 Aluminum which is 276 MPa. In addition to the Von Mises plot, a stress intensity plot was also produced. The stress intensity plot takes into account the 1st, 2nd, and 3rd principal stresses and the discrete plot is given in Figure 5 below.

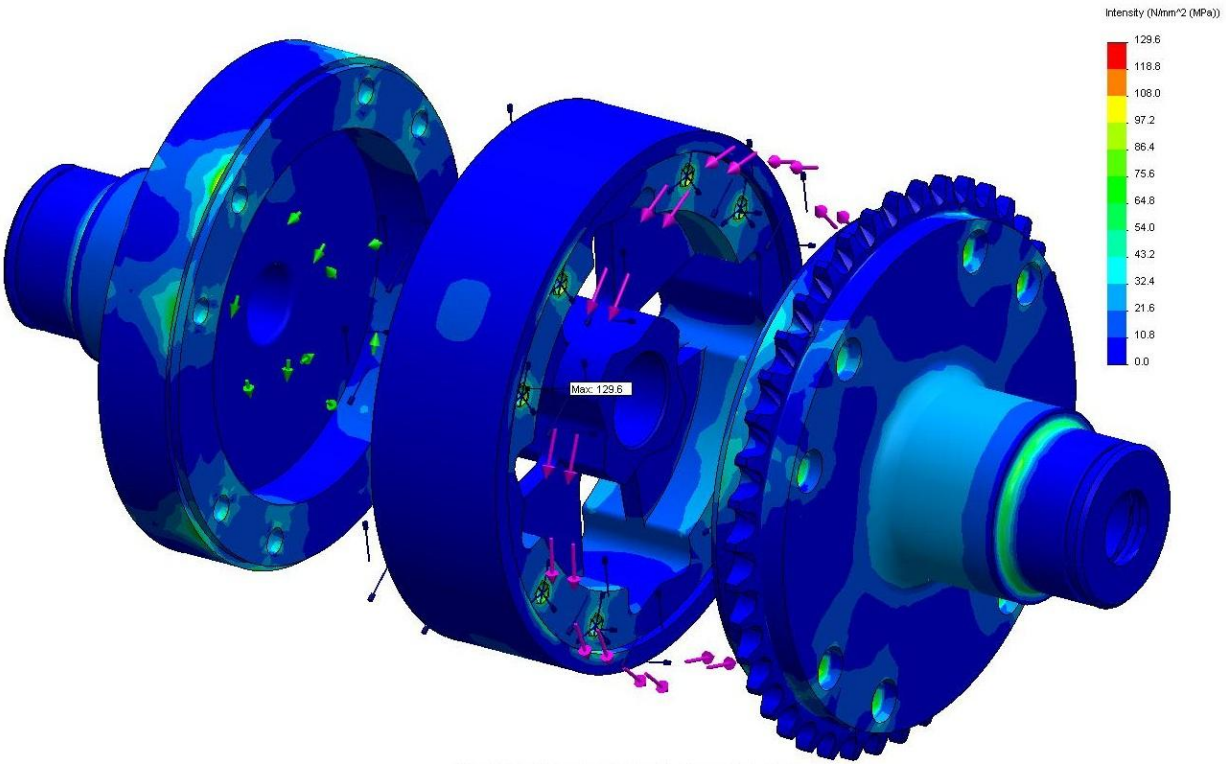

Figure 5: Stress Intensity Discrete Plot

For the stress intensity analysis the location of the maximum stress is located at the thread hole of the carrier and has a magnitude of 129.6 MPa. Like the Von Mises plot, this maximum stress is well below the yield strength for the 1018 Steel which is 370 MPa.

Manufacturing Process and Results

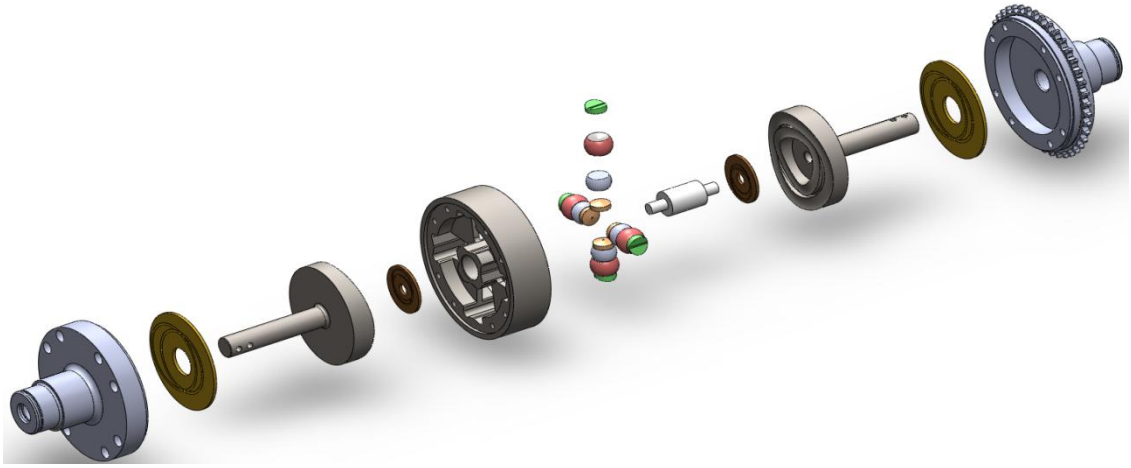

Figure 6: Exploded View of Differential Assembly

There were many bumps along the road to manufacturing parts for the gearless differential. The most prominent of which was having the correct tooling to make the cuts. Along with this was also time management and finding availability of the machine tools needed. A combination of these obstacles made it difficult to cut parts in the time available.

Hubs

The machining of the hubs, although it would appear to be a simple turned part, was impossible without special tooling. The center hole which the cam shaft would turn in had a depth of approximately 3.5 inches, while the longest turning drill available was capable of cutting only 2 inches. This problem could have been resolved by ordering a very pricey drill capable of drilling to the required depth. It was determined that a Kennametal number 3022350 indexable drill with inserts would make the cut possible; however the request for order was late to be approved. Once the center hole was drilled, and the outside profile turned down, the drive

side hub would be mounted in a mill to complete the sprocket teeth. Once the drill needed to make the center hole was acquired, the manufacturing of the hub would go smoothly.

Carrier

The carrier was to be machined out of 6.5 inch diameter 2.15 inch thing 1018 steel round stock. A few changes had to be made in order to machine the part with the available tooling. The radius of the corners on the inside web were originally to be 1/8 of an inch, which would allow the use of a ¼ inch end mill to perform the operation. The pocket needed to be cut to 1.5 inches deep, and all ¼ inch end mills already available were only able to cut to ½ inch deep. A single 3/8 inch end mill was found on hand that could cut to 1.75 inches; so the geometry of the part was redesigned to feature .1875 inch radii.

The carrier was cut on the VF4ss mill; fixtured in a 3-jaw chuck. Being secured at only 3 points, the large cutting forces of a face mill were feared to move the part in the fixture. To avoid this, an open pocketing operation was performed to face the part using a ½ inch end mill instead of the face mill. All went well except the pecking operation to drill the bolt holes on the outside. 4 holes were drilled successfully; however the drill broke making the 5^{th} hole. The broken drill was removed and the rest of the program ran successfully. Total manufacturing time of one side of the carrier was 22 hours. The machined side of the carrier can be seen in Figure 7.
There are several possible reasons for the drill breaking. The flute length may not have been long enough, the peck increment may have been too large, the federate/spindle speed may have been too fast or slow or coolant may not have been clearing the chips and cooling the drill and part properly. If the part was over heating during cutting, it is basically being heat treated. When the

drill comes back down for the next peck it is like cutting into hardened steel, which will cause the tool to break. This problem can be solved by having the drill completely retract from the part and flood with coolant after each peck.

Figure 7: Machined Side of Carrier

Cams

The cams were machined in both the lathe and mill. The roughing of the shaft was completed on the lathe, while the cam face and profile were cut using a mill. It was originally believed that the cam face would need to be cut using 5-axis machining due to the complex geometry of the profile; however it was eventually determined that it could indeed be cut using simple 3-axis technology. After the original program for the cam face was run, burrs were left on either side of the cam profile. A deburring operation was programmed and run on the outside of the cam profile creating an easy fix. The center of the ball endmill also created some defects on the cam surface, however it was so minimal that it was easily removed by polishing. Roughing down the cam shaft end of the cam on the lathe was a 9 hour process, while the machining of the cam face in the mill took 4 hours. The machined cam can be seen in Figure 8.

Figure 8: Machined Cam

Pilot Pin

The Pilot pin was the easiest part to manufacture. The part was simply turned down from round stock. Once fixtured in the lathe, it was simply a matter of roughing the part profile. Once turned down to size, the oil groove was to be machined in a manual mill, however for mass production it could be done in a CNC mill, perhaps using 5 axis technology. Figure 9 shows the machined pilot pin.

Figure 9: Pilot Pin

Bushings

All bushings were machined out of square brass stock. For the center hole and oil grooves, they were fixtured in the mill using standard table clamps around the outside edge, with a sacrificial piece of aluminum underneath to allow clearance for the through hole without collision with the table. Once these features were cut, the bushings were fixtured using a bolt through the center hole to allow the outside circumference to be cut. Once again a piece of sacrificial aluminum was used underneath. Figure 10 shows a machined bushing. The first bushing that was cut had one problem; the outside diameter was too small. It was determined that the problem was due simply to not accounting for the radius of the tool in the CAM programming.

Figure 10: Machined Cam Bushing

Sliding Ball Bearings

The manufacturing of the internal ball bearings which are responsible for allowing differentiation proved to be a feat. Since the bearings are hardened, it is very difficult to remove material from them. A fixture was made to allow the spherical bearings to be ground down. The process was incredibly long, taking off only a fraction of a thousandth of an inch of material for each pass. The correct dimensions of the balls were attained in this manner; however the machining of the bearing caused the part to lose its hardness in that area. Due to the function of the part, it is paramount that those surfaces be hardened. The original configuration of the bearings is shown in Figure 11.

Figure 11: Altered Ball Bearings (Tsiriggakis, 2003)

The possibility of using an outside vendor to manufacture the part was researched, however it was found to be prohibitively pricey. All balls for one differential were priced around $1700, which was out of the projects budget scope. If it were to be done again, the possibility of having the balls rehardened or specially coated after in house machining would be explored.

Internal and External Frame mounts

Although the frame mounts were never cut, a manufacturing process was determined. Both parts would be cut using a CNC lathe. One side would be faced and internal features cut, and then turned around in the spindle and the other side faced and features cut. The outside mounting holes were to be cut using live tooling so that all operations could be cut on the lathe.

Live tooling is simply the use of a powered, spinning tool holder allowing holes to be drilled while the part remains still in the lathe spindle.

Frame Alterations

In order to place the pre assembled differential into frame, a section of the frame would need to be removed. Figure 12 shows the section of the frame to be removed and altered to bolt back in its existing location. In order to do this, the current mounting flange for the drive train would need to be removed. This would be accomplished by simply grinding off the welds using a cut off wheel. If the flanges were removed without damage, they would simply be welded back on to the outside of the frame, rather than inside. If they were damaged, new flanges would be machined in a mill using plate steel. The removed section of the frame would be fitted with a pin at one end, and a flange welded at the other to fixture back to its original location, allowing the differential to be removed when needed.

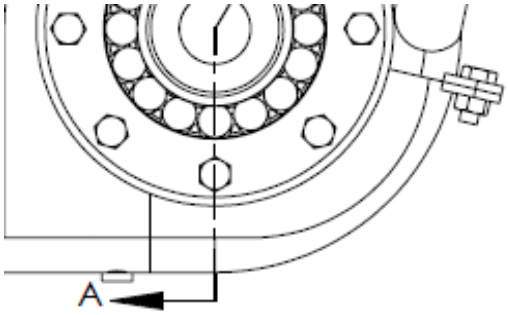

Figure 12: Section of Frame to be Removed

Recommendations for Machining

If this project were to be done again, machining of parts would definitely start earlier. It is almost always true with any design project that machine time is going to take twice as long as originally intended. There are so many unforeseen obstacles on the path to a completed part. The tooling needed to cut the part may not be readily available, there may be problems with the G code written for the part, tooling may break or wear, machine tools may not be available when needed etc. By getting an early start on manufacturing many of these problems may not be avoided, but a deadline can still be met while overcoming them. A photo of the carrier, cam and bushing assembled can be seen in Figure 13.

Figure 13: Carrier, Cam, and Cam Bushing

Conclusions and Recommendations

This report has discussed the development of a gearless differential for the SAE Baja vehicle. The objectives were to design a differential to replace the existing solid axle setup and allow the car to corner more efficiently under power. The differential also had to be a gearless type differential due to the lack of manufacturing resources available. Being an off-road vehicle, the differential also needed to posses certain traction controlling characteristics either in the form of limited slip or locking. The differential also needed to be race-ready and increase the performance of the vehicle, although not for the 2010 vehicle, but for next year's competition vehicle. Not all objectives were met; in part because production is incomplete, postponing installment into the vehicle and showing whether or not the differential works as expected.

Progression from theoretical design to manufacturing and assembly of a gearless differential has shown how difficult it is to produce a finished prototype. Without the results of any kind of field testing it's difficult to say whether this differential is capable of performing to the capacity expected. Thorough research of the original inventor of the differential, Tsiriggakis, shows that it's been tested in full scale automobiles. Analysis and testing would also have been a solid basis for more refined materials selection. In designing the differential, numerous factors need be considered along the way each one altering the design. Whether it is accounting for different loading conditions, or proper lubrication, each change proved to be difficult, as much of the design had to be altered to account for the changes. Machining the components of this differential proved simpler than expected. Minimal setbacks such as incorrect stock selection and tool breakages have impeded the production slightly, but weren't enough to halt the process. Manufacturing will continue and likely be finished in the beginning of next year which will leave ample time for thorough lab and field testing.

Recommendations for further development of this gearless differential would include extensive testing into the capabilities and limits by subjecting the differential to numerous, strength and operational tests. These tests would be able to indicate any kind of wear issues, inefficiencies within the differential, as well as any kind of subsequent losses due to variations of internal structure. Testing would gauge the differentials resiliency to large applied torques in different scenarios.

Before the differential is even implemented into the vehicle the differential can be setup in a simple jig that lets the differential rotate freely. This would allow for simple operational analyses to be performed showing whether the differential works under minimal conditions. The differential would sit between two rings attached to a stationary platform. These rings would be dimensioned around the bearings and the differential would seat in between these two rings. The differential is free to rotate in between the rings. Then, round weights similar to the weight of the wheels on the Baja vehicle can be attached to shorter half shafts. The differential can then be spun by hand or attached to a motor/locomotion source via chain and sprocket to show if the wheels spin in the direction of the differential. Alternatively, the differential can be spun while friction is applied to either wheel to simulate cornering and visual analysis of the free wheel will show if differentiation is unimpeded. This test is simple, but shows the basic operation of the differential under a range of torques and conditions.

Implementation of the differential into the vehicle can be considered. This allows for further performance testing in the vehicle. One possible test could simulate start-line instantaneous applied torque, where the car is at complete standstill. Then, full throttle is applied instantaneously for a short period of time and then full brakes. This test would simulate extreme operating conditions, start-stop conditions. This test should be repeated numerous times to define the limits of the differential in extreme situations. Following the disassembly of the differential, examination of the wear that these conditions have on the components would show the resiliency of the design to the harshest of conditions. Not only can start-stop conditions be examined, but also a simulated race to see the wear of one race period.

Other testing could include suspending both rear drive wheels, allowing them to free-spin at full power, and then suddenly apply brake to one of the wheels. This test would simulate the rock-crawling aspect of the competition where often one wheel is suspended and free spinning while the other is in contact. Traction testing can also be done with various surface conditions to see how much actual slip there is with the differential. This test would encompass placing the vehicle on varying surface conditions; mud and loose sand where grip is very minimal, wet pavement and dry pavement where grip is higher but the wet pavement provides a slipperier surface. The surface can also be put side by side with mud under one wheel and pavement under the other. Video analysis of both wheels would show whether the differential is able to move the vehicle forward without plunging the wheel in mud further down.

These tests can then be repeated for variations within the internal structure of the differential. The amplitudes of the sinusoidal cams can be altered to see the effect on slip conditions. The sizing of the ball bearings can also be altered to see the effect of larger/smaller contact area between the ball bearing and the tracks of the face cams. This would show how much friction loss there is within the differential in comparison to a traditional geared differential where tooth geometry and gear mesh dictate losses. Differential fluid selection can therefore become a measure of the effect of the fluid viscosity on the efficiency of the differential. By selecting different fluids it can be seen whether higher or lower viscosity fluids improve the performance of the differential while maintaining proper wear characteristics.

Further analyses of these tests would provide evidence as to the ability of this differential. Examination of the differential's functioning capability would show if the sinusoidal cam tracks

allow differentiation of the wheels as well as limiting slip under straight line power. If it doesn't, then the internal geometry of the differential has to be reconfigured to accommodate for this. Analyses of the strength tests would show the benefit of implementing a gearless differential over a gear type differential where gear tooth failure is often catastrophic. If the differential holds up under similar operating conditions, then its practicality is supported with its simpler design. Performance testing is practical, but shows the various surface conditions that this vehicle could encounter. This type of testing would also prove the differentials ability on all types of surfaces, showing its versatility in numerous applications other than the SAE Baja vehicle. This would of course, be beneficial in regards to the SAE Baja competition where the vehicle competes in numerous events with extremely varied conditions. Only after the testing described herein is performed, can the determination of whether to use the differential in the vehicle during competition be made.

Bibliography / Vendor Information

Banovics, Aaron. Das Kugeldifferential-Google Translate. 2005. 20 April 2010 <http://translate.google.com/translate?hl=en&sl=de&tl=en&u=http%3A%2F%2Fwww.offroad-cult.org%2FSpecial%2FKugeldifferential%2FDiff.htm>.

Burnhill, Darren. Model Car Differentials-The Ball Differential. 2009. 20 April 2010 <http://www.rctek.com/technical/differentials/ball_description.html>.

Differential. 2010. 20 April 2010 <http://www.yourautonetwork.com/differential.html>.

Norton, Robert L. *Design of Machinery: an Introduction to the Synthesis and Analysis of Mechanisms and Machines*. 4th ed. Dubuque, IA: McGraw-Hill, 2008. Print.

Norton, Robert L. *Machine Design: an Integrated Approach*. 3rd ed. Upper Saddle River, N.J.: Pearson Prentice Hall, 2006. Print.

Oberg, Erik, et al. Machinery's Handbook 28th Ed. New York: Industrial Press, 2008.

Tsiriggakis' Gearless Differential, http://www.tsiriggakis.gr/gd.html, 2003.

Tsiriggakis, Theodoros. United States Patent # 4,509,388: Differential Gear. April 9th, 1985

Material Property Data. 2010. 15 March 2010 <http://www.matweb.com/>.

All Stock from:

Peterson Steel

61 West Mountain Street

Worcester, MA 01606-1342

(508) 853-3630

www.petersonsteel.com

Bearings from:

Timken

Motion industries

(508) 229 2688

Photos by Justin Goodwin

Models and drawings created with:

SolidWorks 2009

Calculations done using MathCAD14

NC Code written with Esprit 2010

Machine tooling from Kennametal Inc.

Appendix A: Bill of Materials and Chassis Assembly

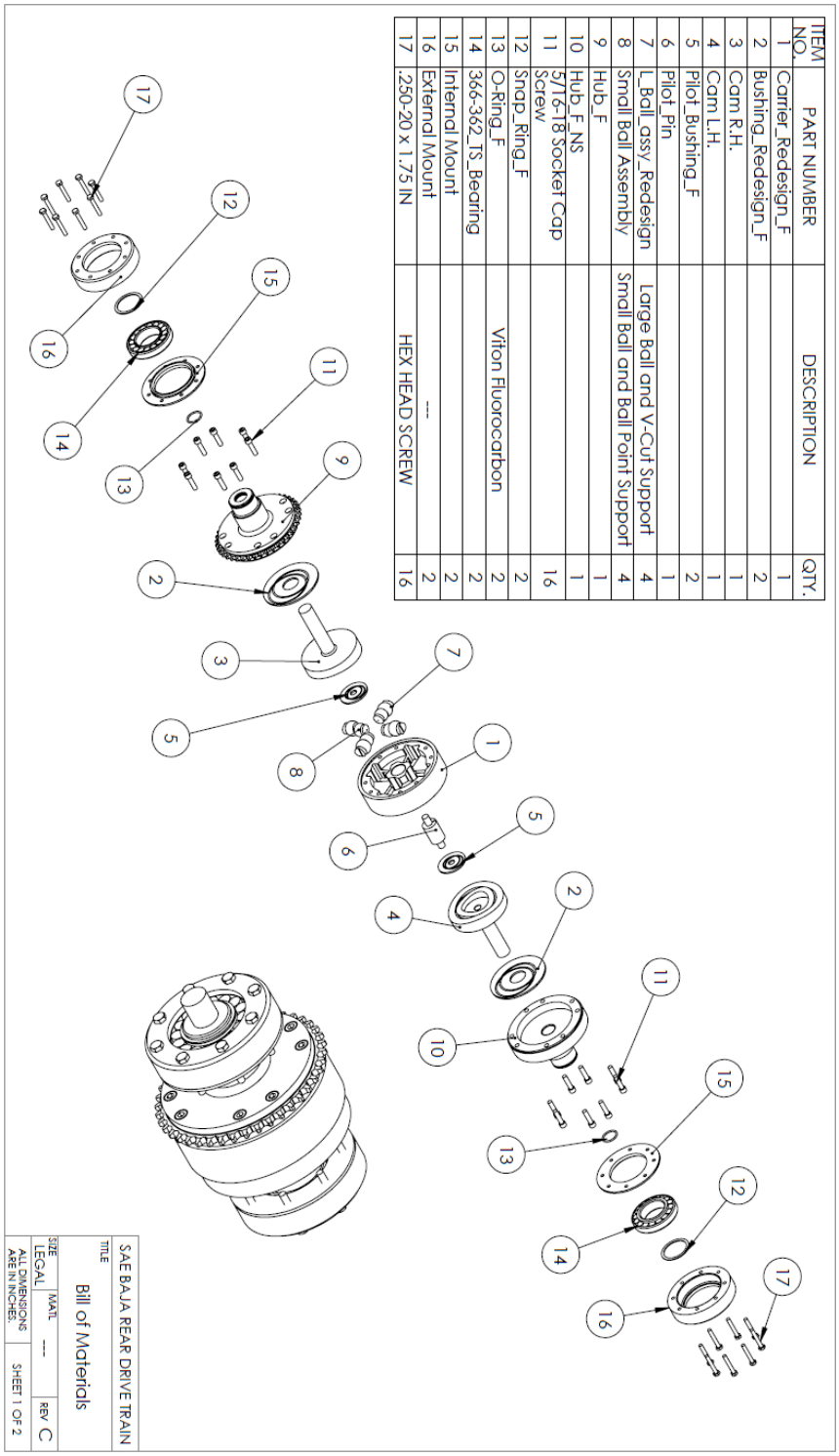

ITEM NO.	PART NUMBER	DESCRIPTION	QTY.
1	Carrier_Redesign_F		1
2	Bushing_Redesign_F		2
3	Cam R.H.		1
4	Cam L.H.		1
5	Pilot_Bushing_F		2
6	Pilot_Pin		1
7	L_Ball_assy_Redesign	Large Ball and V-Cut Support	4
8	Small Ball Assembly	Small Ball and Ball Point Support	4
9	Hub_F		1
10	Hub_F_NS		1
11	5/16-18 Socket Cap Screw		16
12	Snap_Ring_F		2
13	O-Ring_F	Viton Fluorocarbon	2
14	366-362_TS_Bearing		2
15	Internal Mount	---	2
16	External Mount		2
17	.250-20 x 1.75 IN	HEX HEAD SCREW	16

SAE BAJA REAR DRIVE TRAIN

TITLE: Bill of Materials

SIZE	MAT'L	REV
LEGAL	---	C

ALL DIMENSIONS ARE IN INCHES.

SHEET 1 OF 2

ITEM NO.	PART NUMBER	DESCRIPTION	QTY.
1	Baja Chassis		1
2	RH_Rear-End_Pipe_Joint		1
3	LH_Rear-End_Pipe_Joint		1
4	.250-20 x .625 IN	HEX HEAD SCREW	2
5	.250-20 UNS	HEX NUT	2

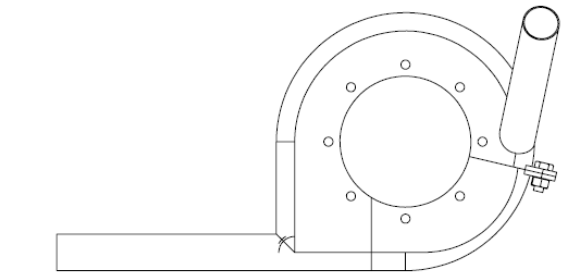

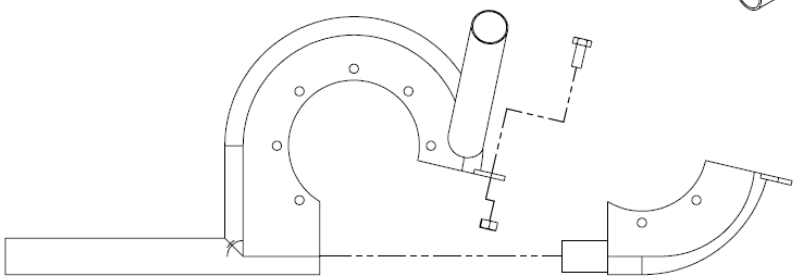

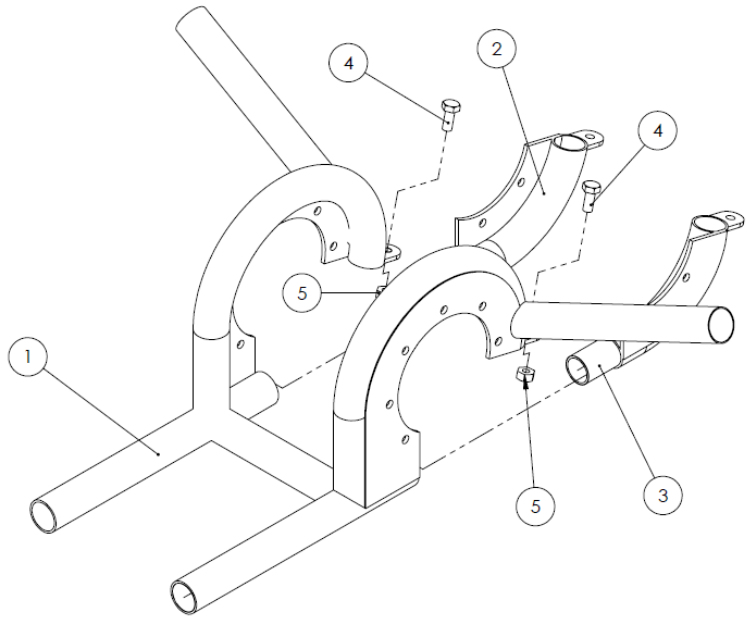

SAE BAJA REAR DRIVE TRAIN

TITLE
Chassis Assembly

SIZE	MATL	REV
LEGAL	---	C

ALL DIMENSIONS ARE IN INCHES.

SHEET 2 OF 2

Appendix B: Differential Assembly

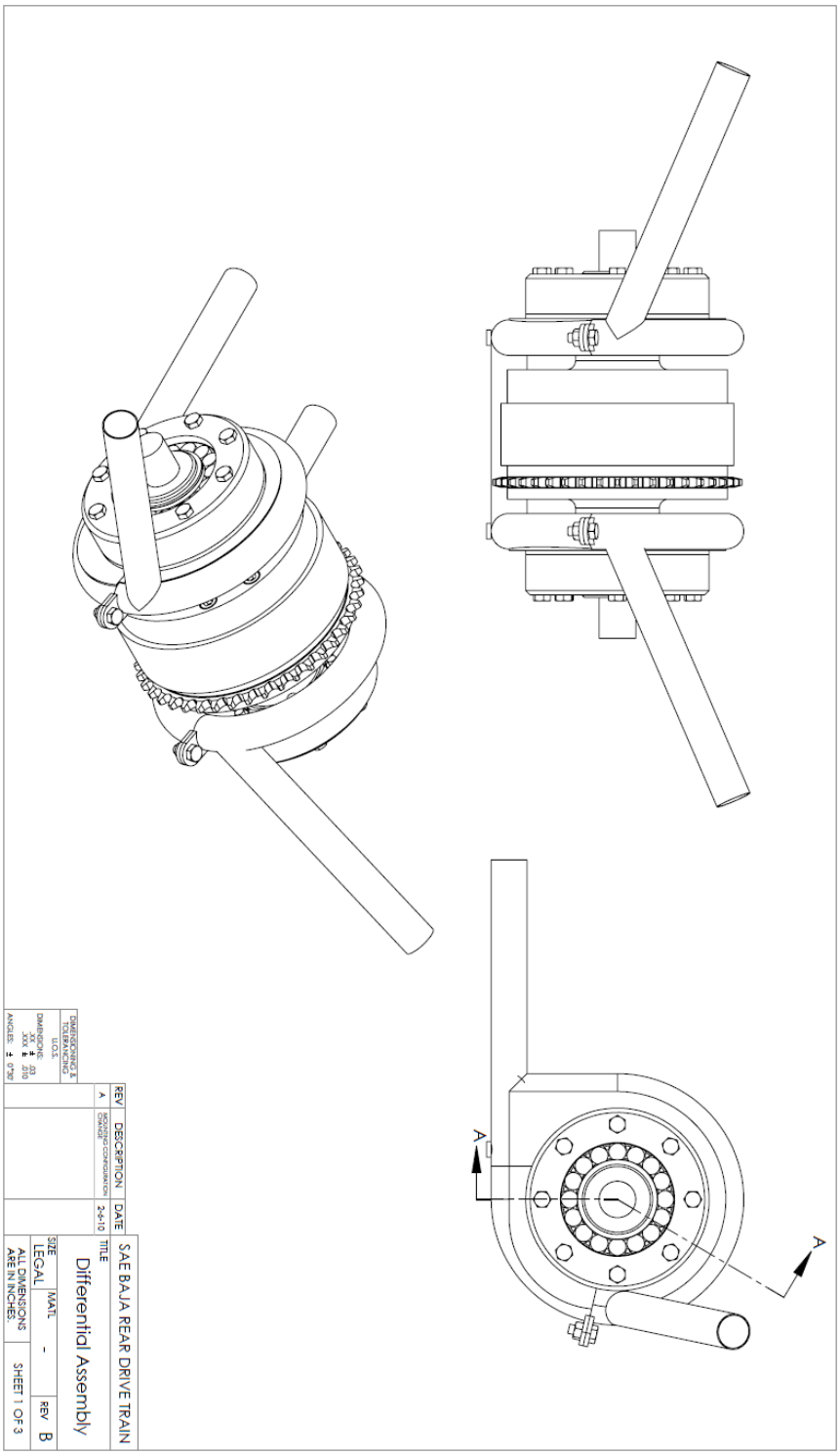

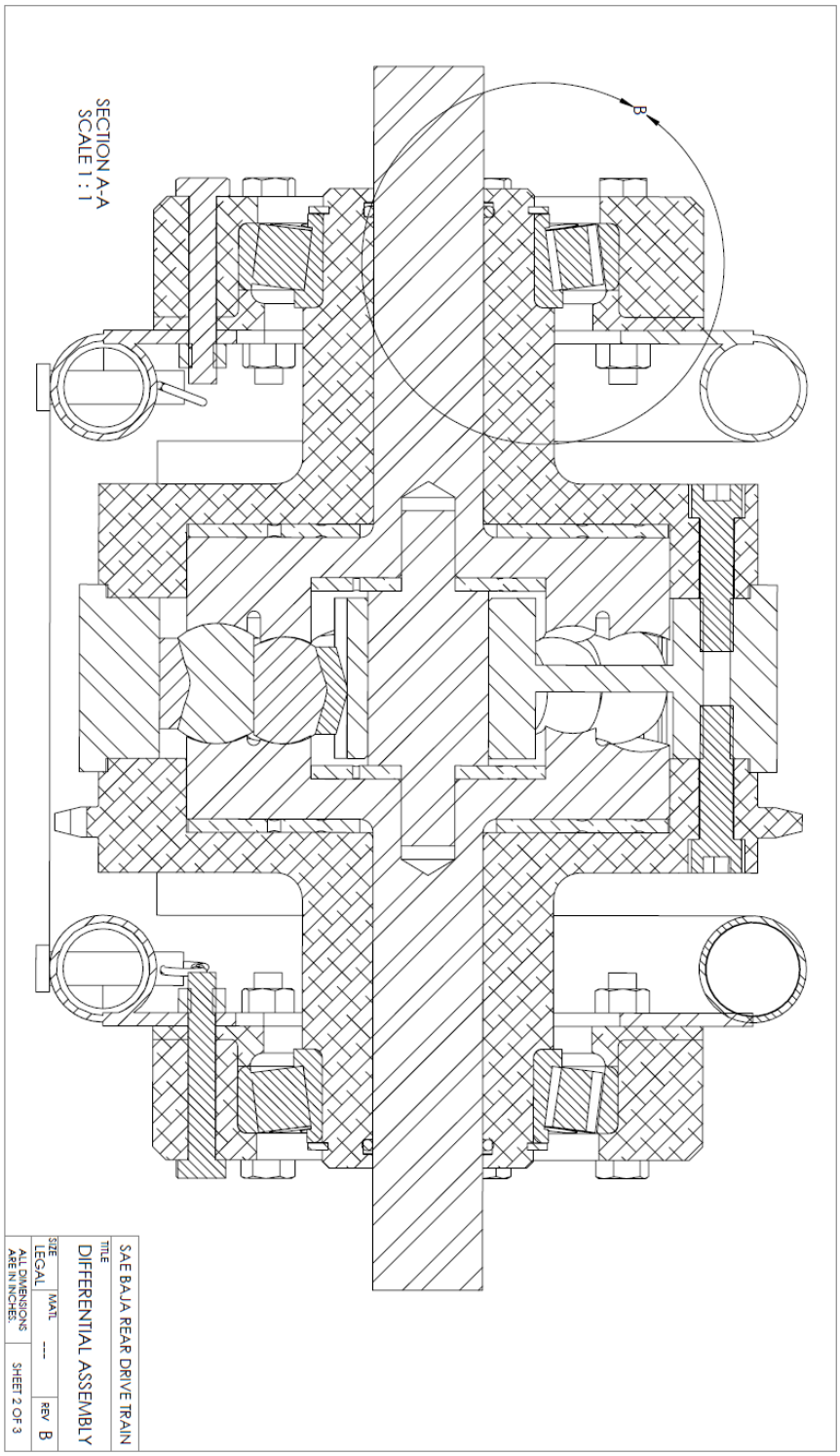
SECTION A-A
SCALE 1 : 1
B
SAE BAJA REAR DRIVE TRAIN
TITLE
DIFFERENTIAL ASSEMBLY
SIZE
LEGAL
MATL

REV B
ALL DIMENSIONS ARE IN INCHES.
SHEET 2 OF 3

ITEM NO.	PART NUMBER	DESCRIPTION	QTY.
1	Baja Chassis		1
2	Internal Mount		2
3	External Mount	---	2
4	.250-20 UNS	HEX NUT	18
5	Differential_Assembly		1
6	.250-20 x 1.75 IN	HEX HEAD SCREW	16
7	Timken 366-362 Bearing		2
8	Snap Ring		2
9	O-Ring		2

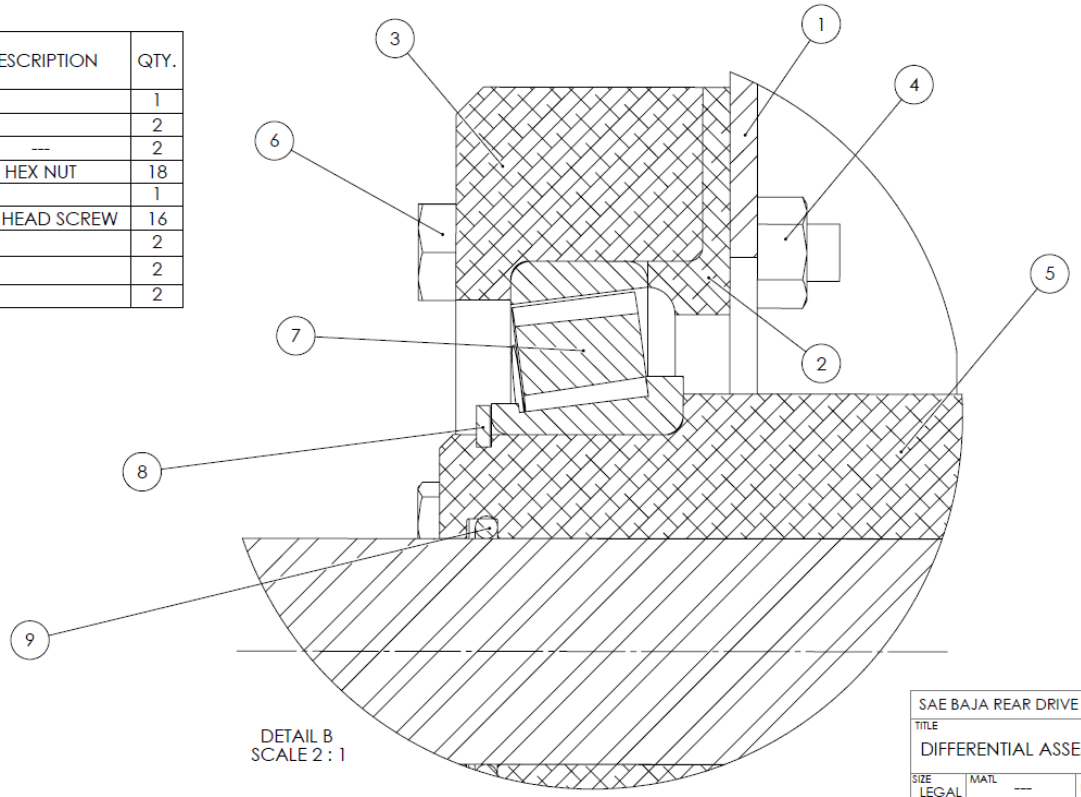

DETAIL B
SCALE 2 : 1

SAE BAJA REAR DRIVE TRAIN

TITLE
DIFFERENTIAL ASSEMBLY

SIZE	MATL	REV
LEGAL	---	B

ALL DIMENSIONS ARE IN INCHES.

SHEET 3 OF 3

Appendix C: Hub (No Sprocket)

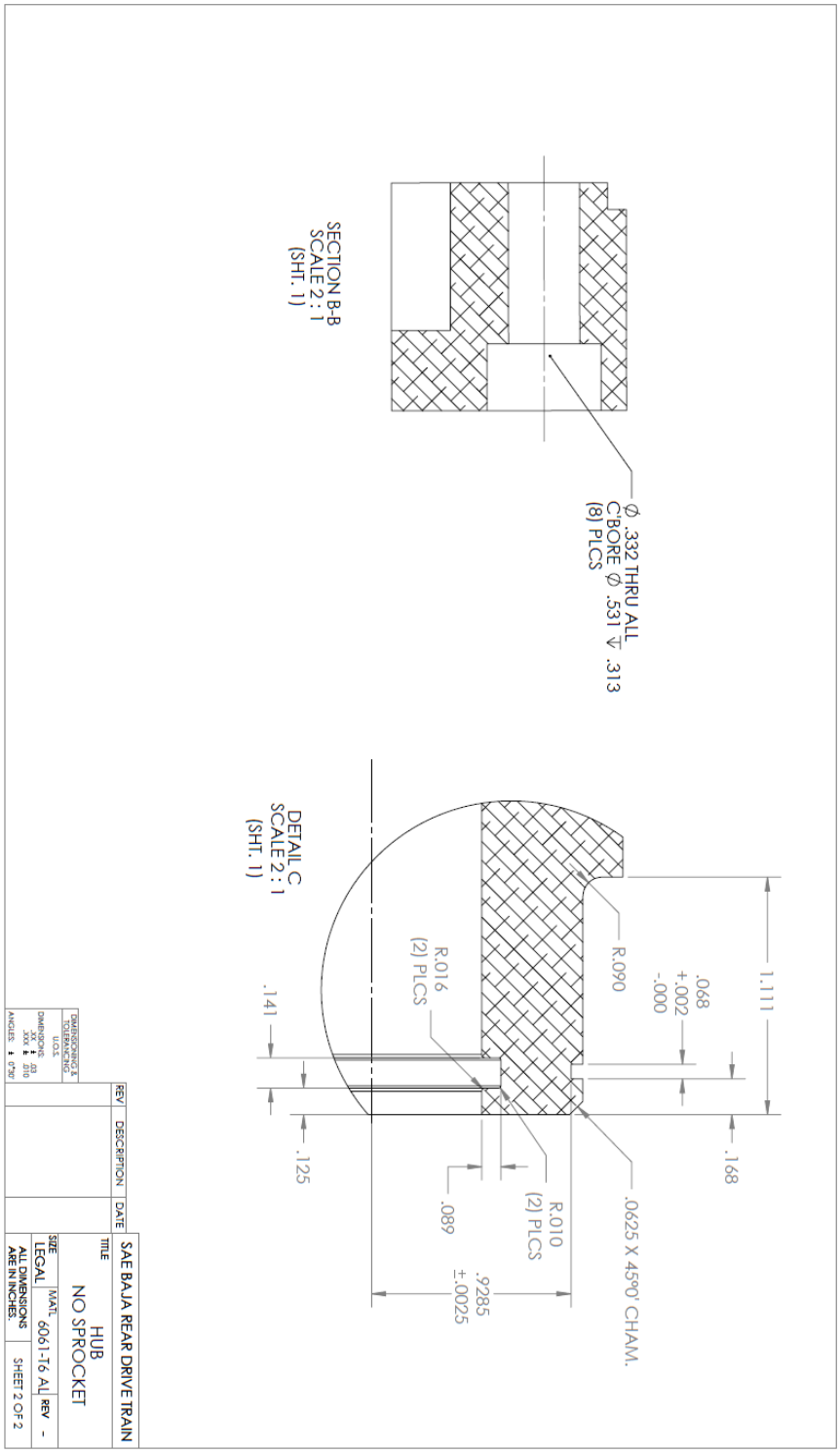

Appendix D: Cam Bushing

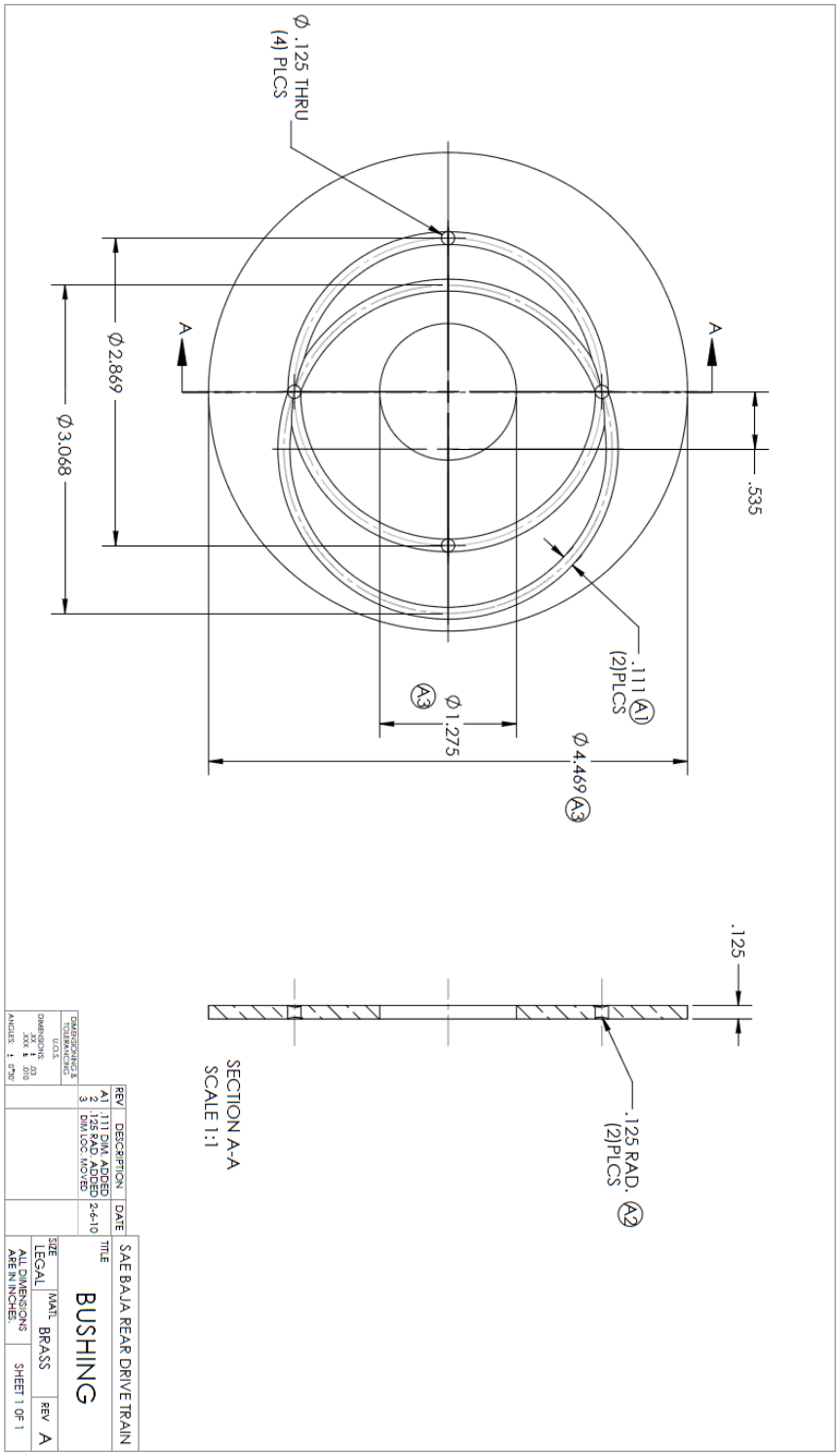

Appendix E: Cam (Left Hand)

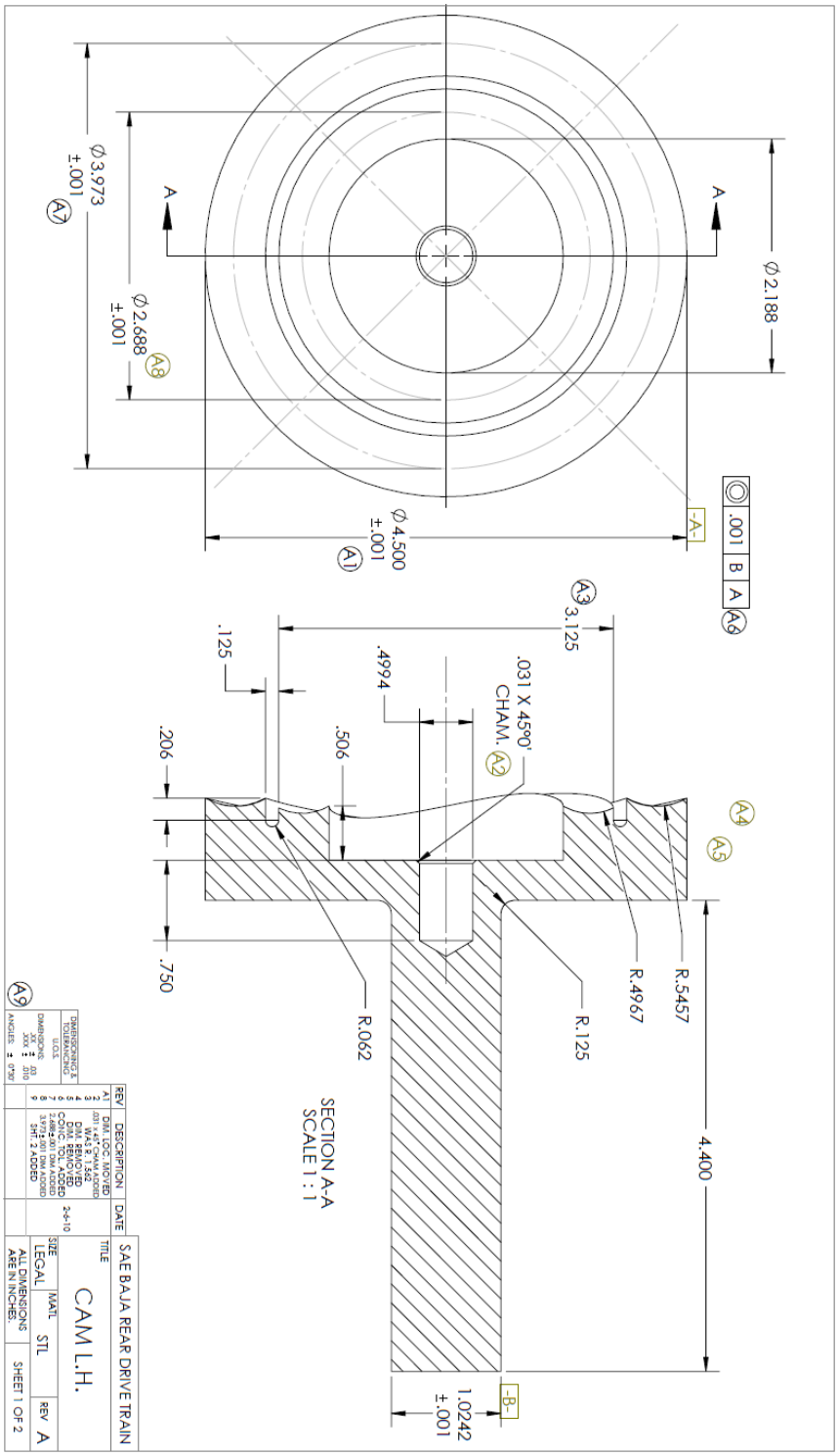

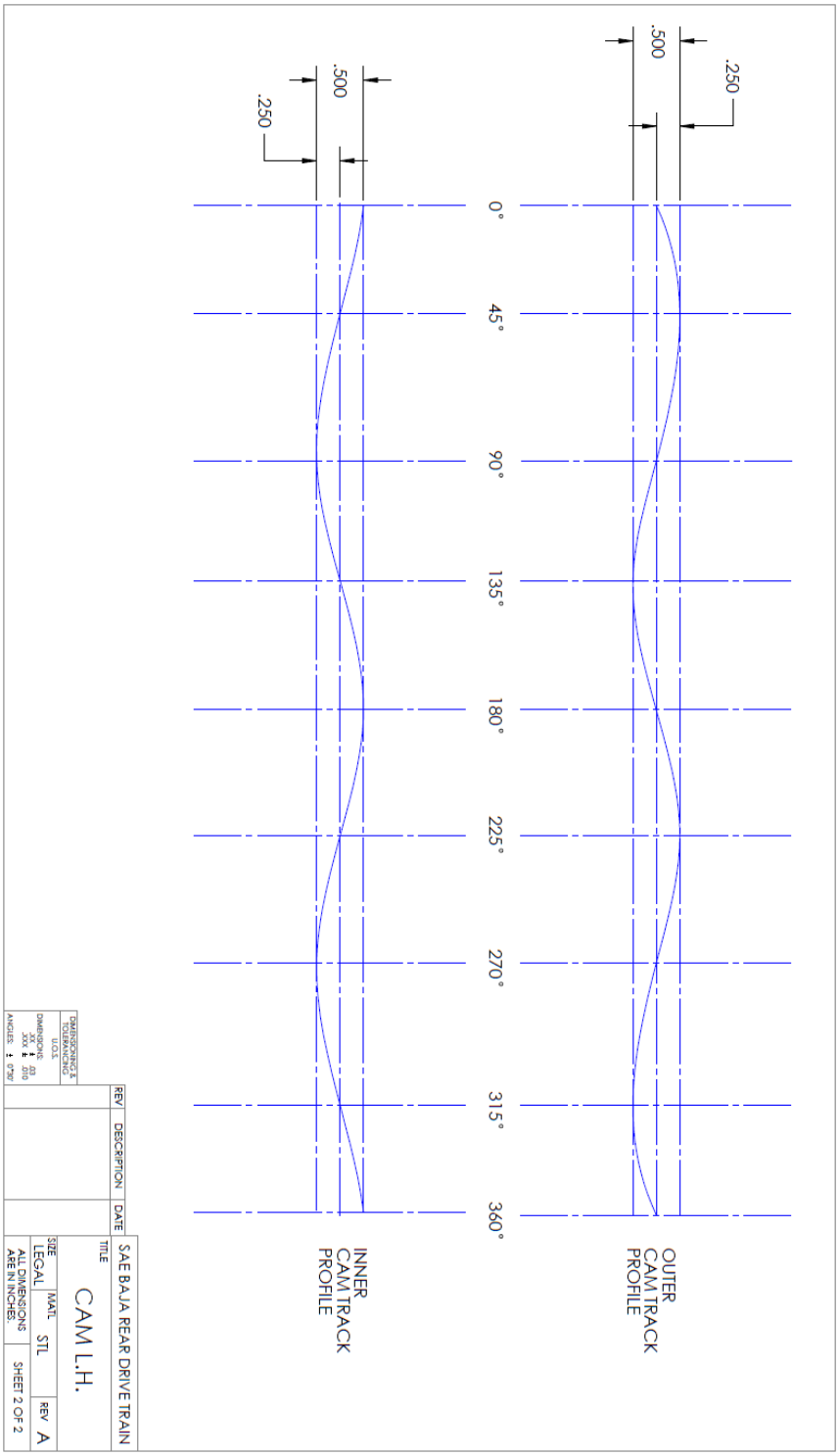
.250
.500
.500
.250
0°
45°
90°
135°
180°
225°
270°
315°
360°
OUTER CAM TRACK PROFILE
INNER CAM TRACK PROFILE
DIMENSIONING & TOLERANCING
U.O.S.
DIMENSIONS .03
XXX ± .010
ANGLES ± 0°30'
REV
DESCRIPTION
DATE
TITLE
SAE BAJA REAR DRIVE TRAIN
CAM L.H.
SIZE
LEGAL
MAT'L
STL
REV
A
ALL DIMENSIONS ARE IN INCHES.
SHEET 2 OF 2

Appendix F: Pilot Bushing

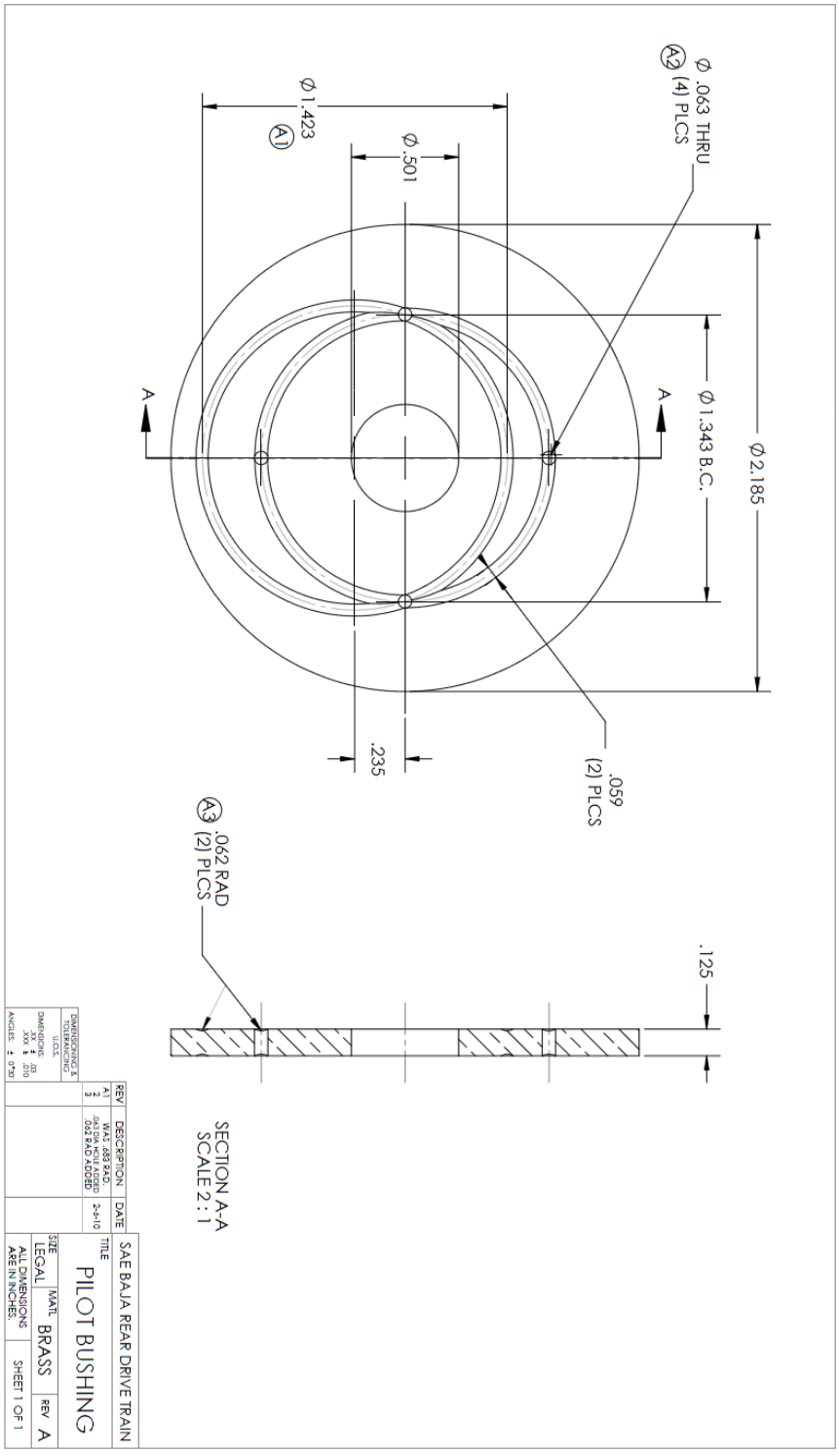

Appendix G: Carrier

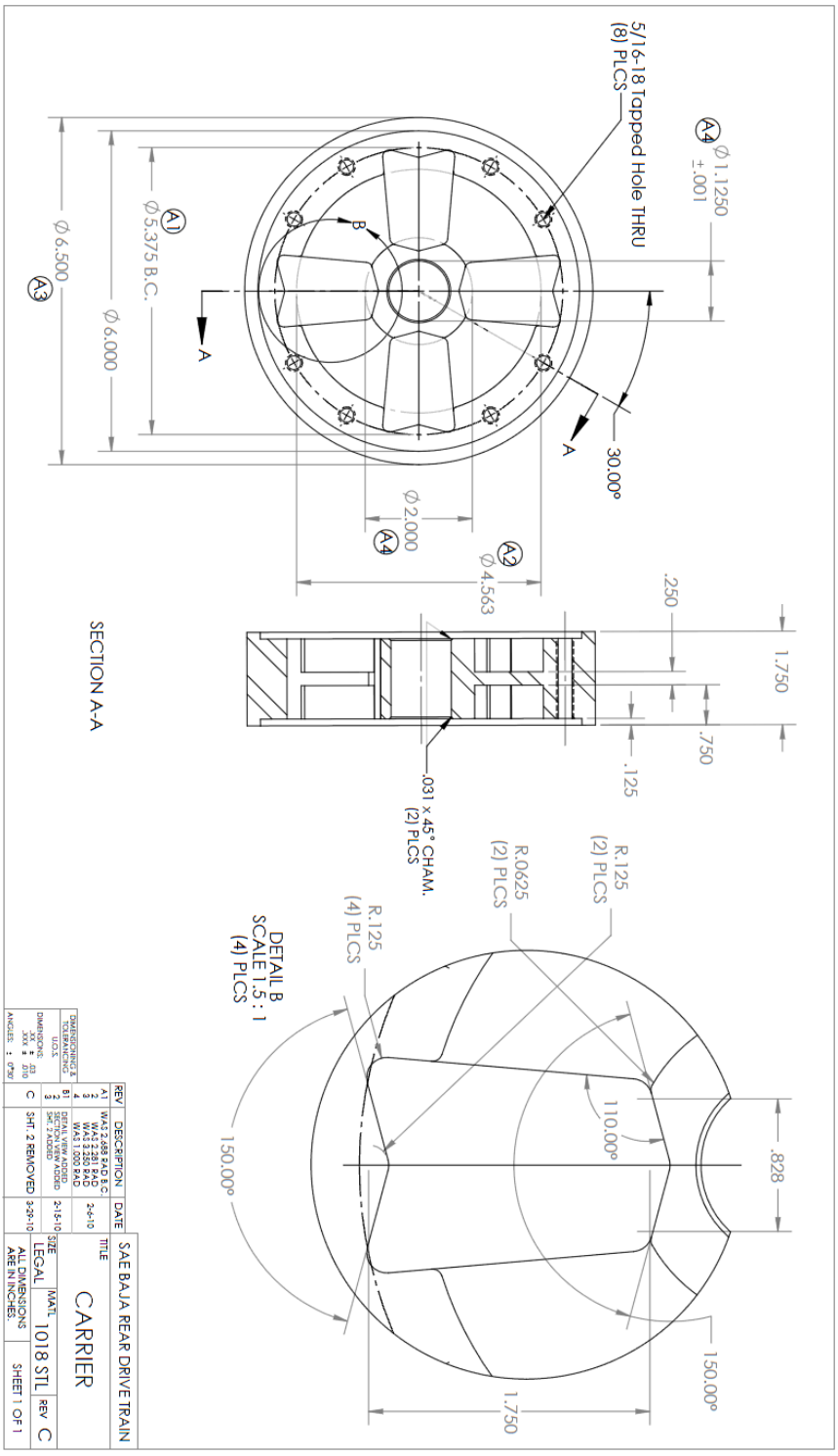

Appendix H: Ball Point Support

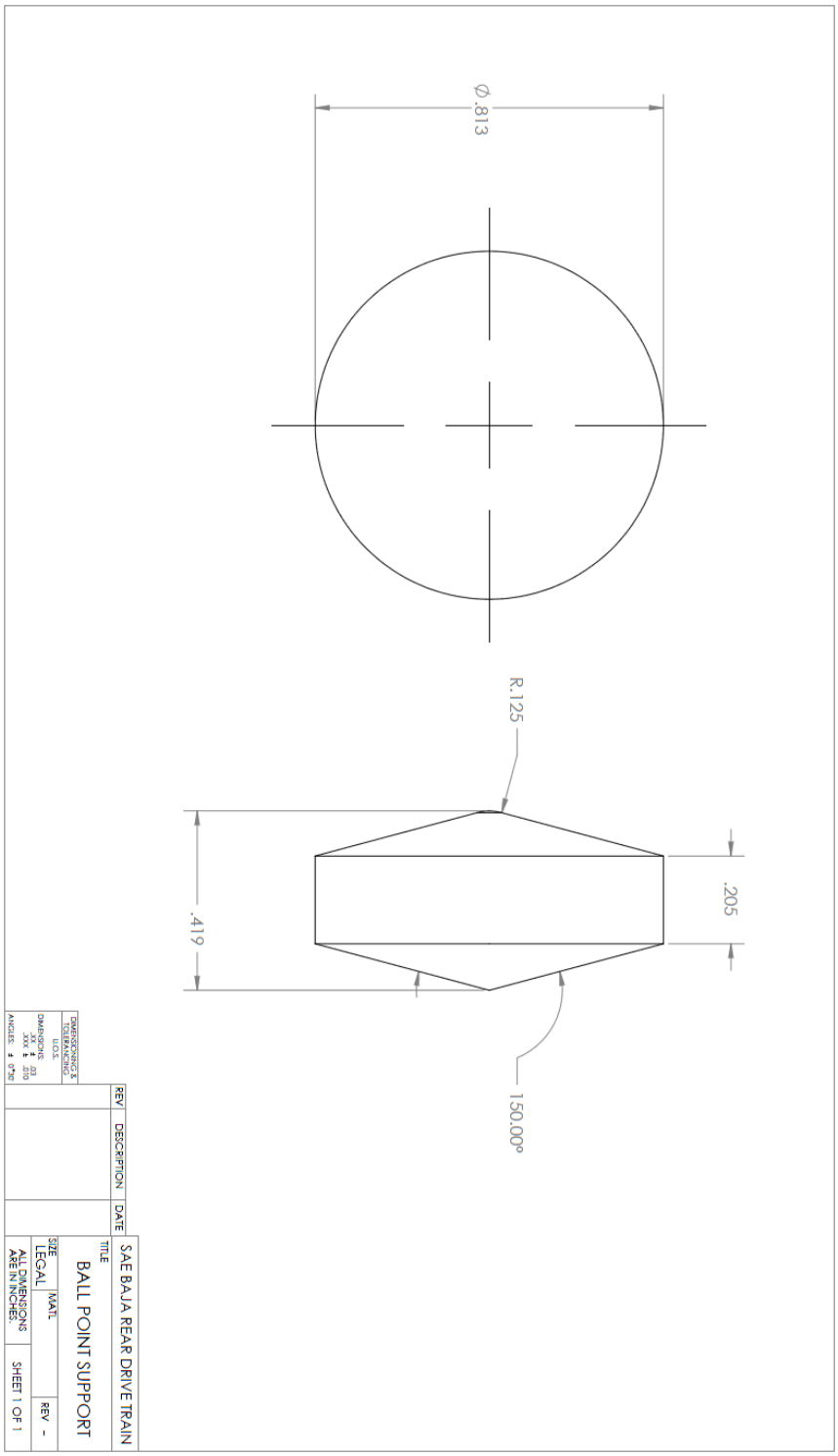

Appendix I: Inner (Small) Ball

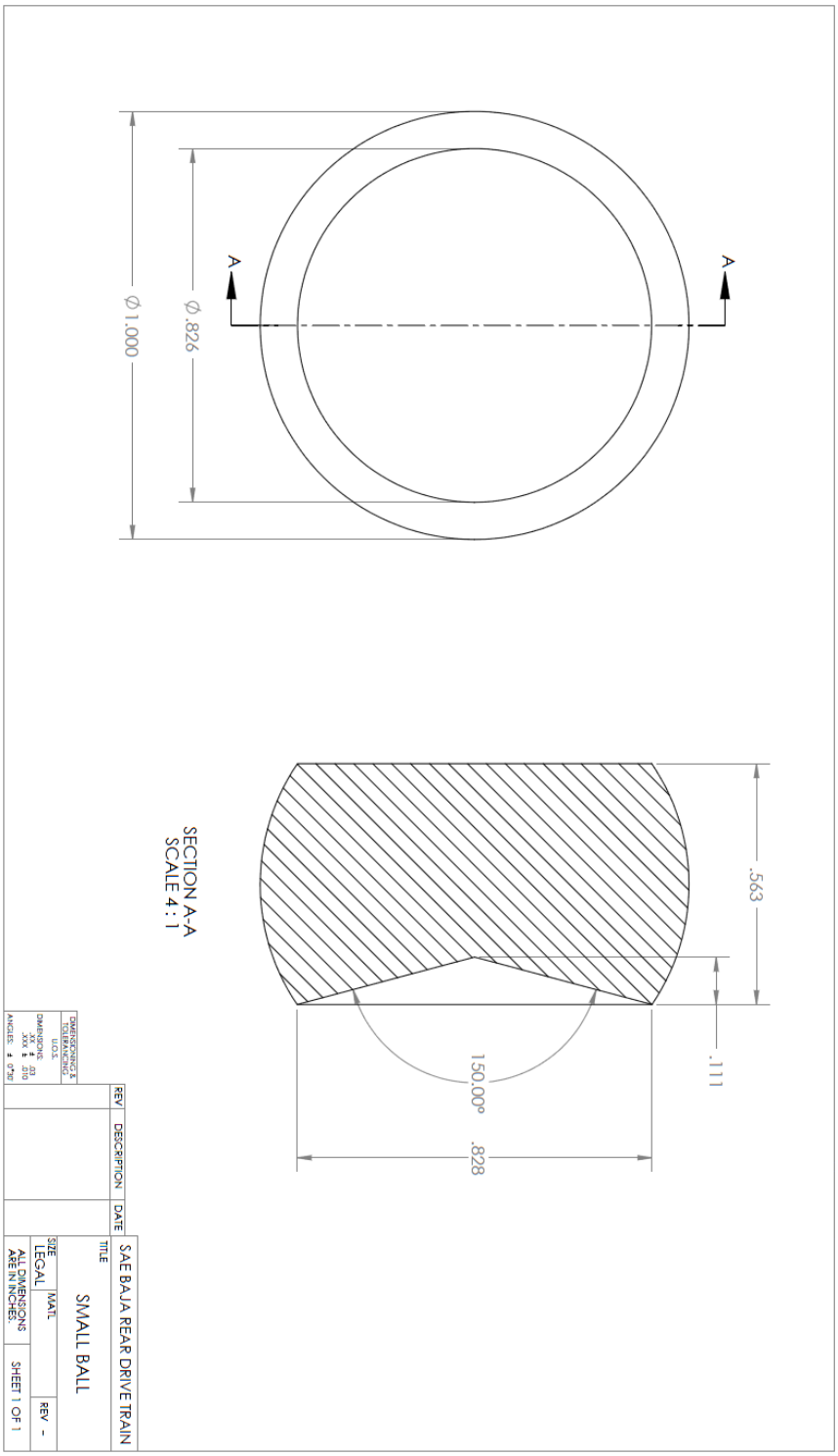

Appendix J: Outer (Large) Ball

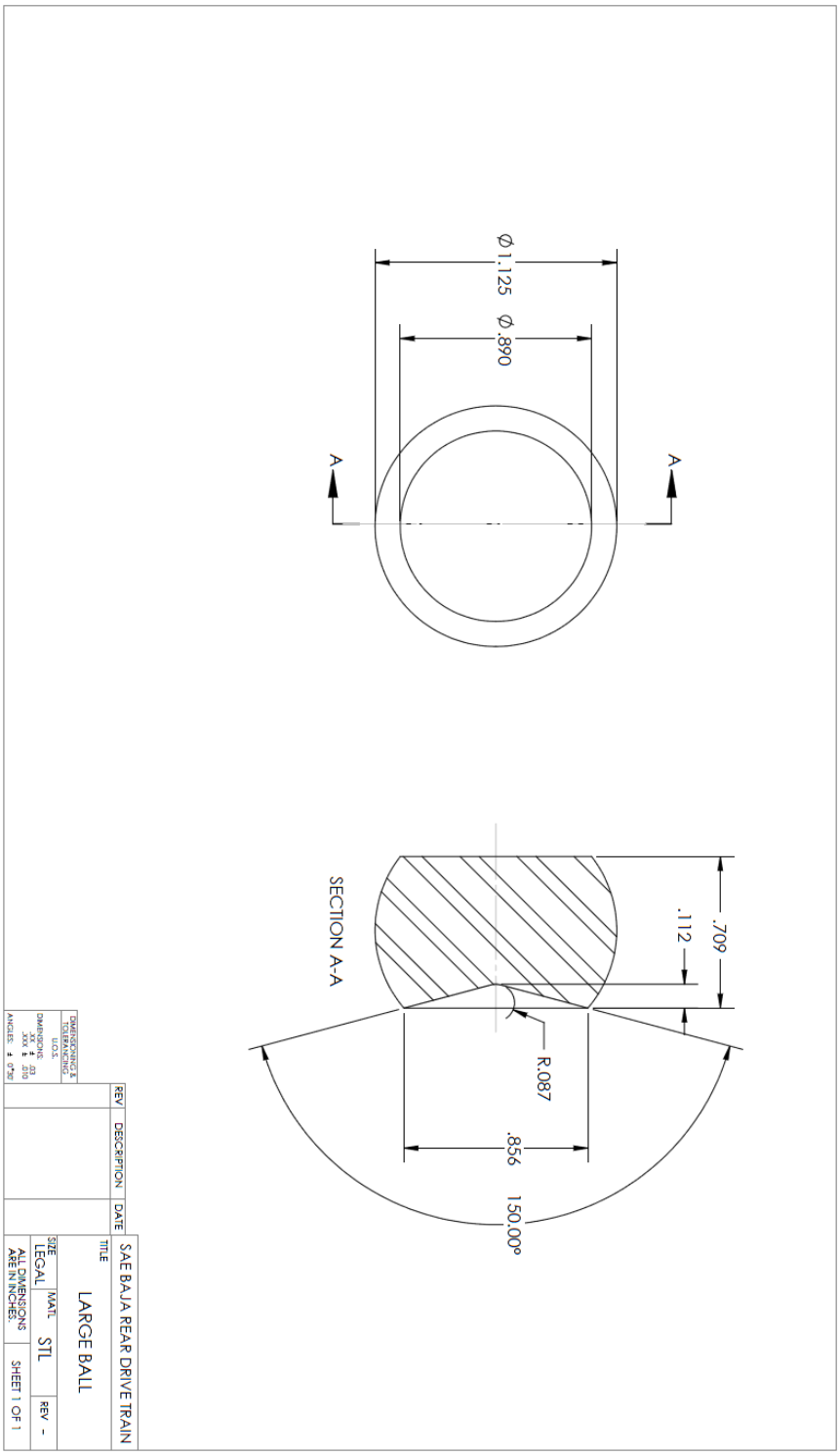

Appendix K: V-Cut Ball Support

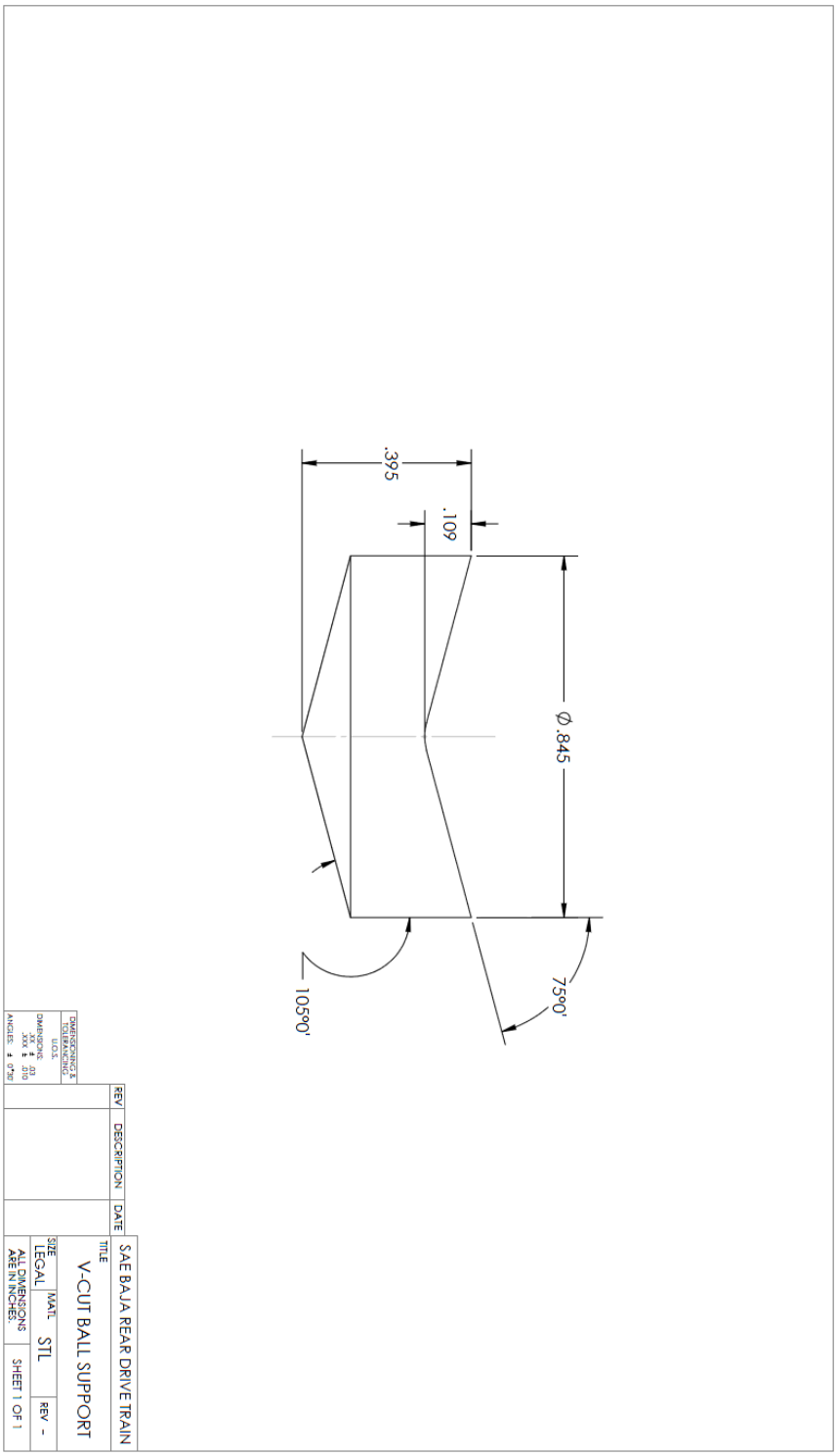

Appendix L: Pilot Pin

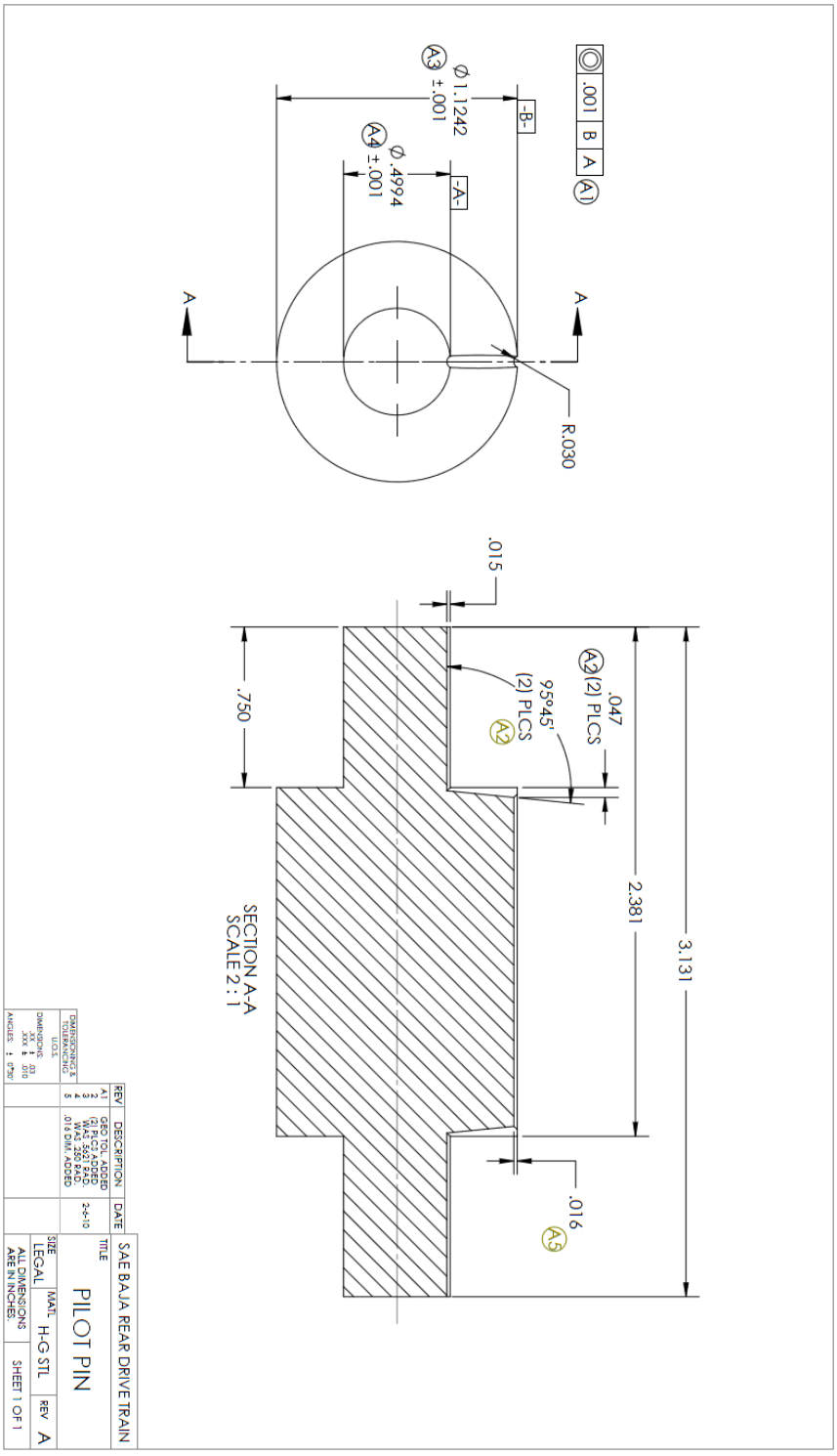

Appendix M: Cam (Right Hand)

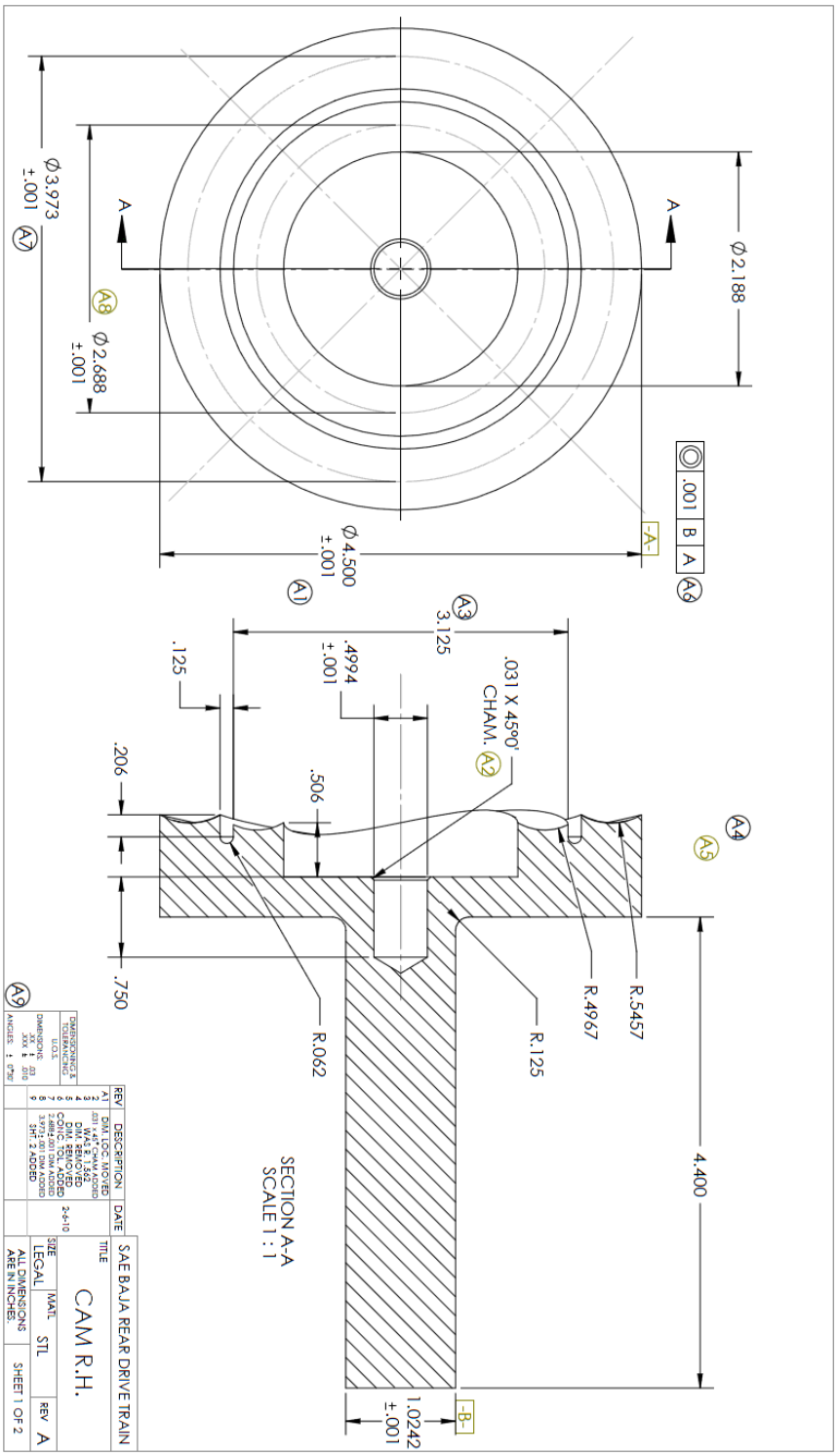

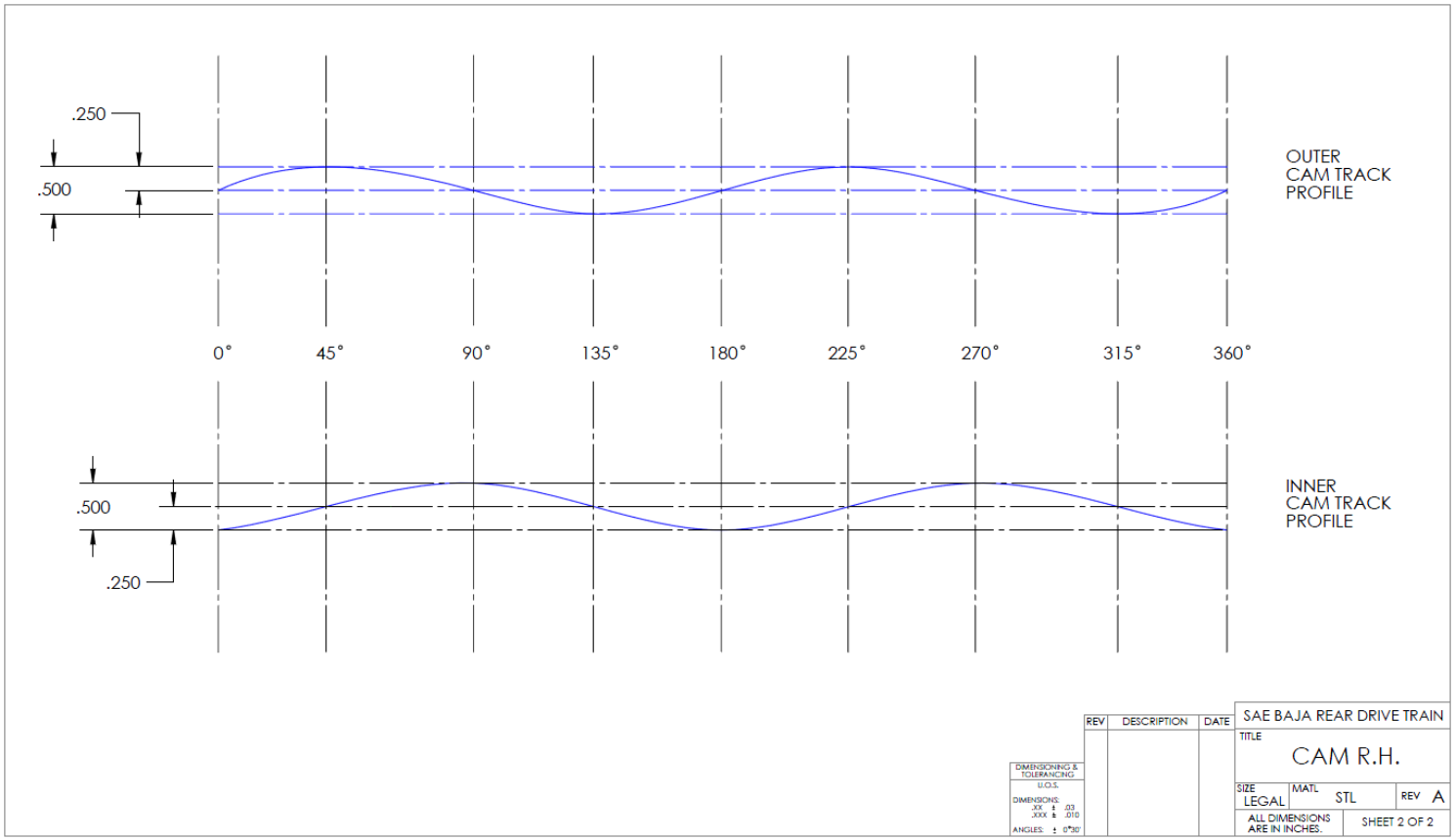
.250
.500
OUTER
CAM TRACK
PROFILE
0°
45°
90°
135°
180°
225°
270°
315°
360°
.500
.250
INNER
CAM TRACK
PROFILE
REV
DESCRIPTION
DATE
SAE BAJA REAR DRIVE TRAIN
TITLE
CAM R.H.
DIMENSIONING & TOLERANCING
U.O.S.
DIMENSIONS:
.XX ± .03
.XXX ± .010
ANGLES: ± 0°30'
SIZE
LEGAL
MATL
STL
REV A
ALL DIMENSIONS ARE IN INCHES.
SHEET 2 OF 2

Appendix N: Hub (With Sprocket)

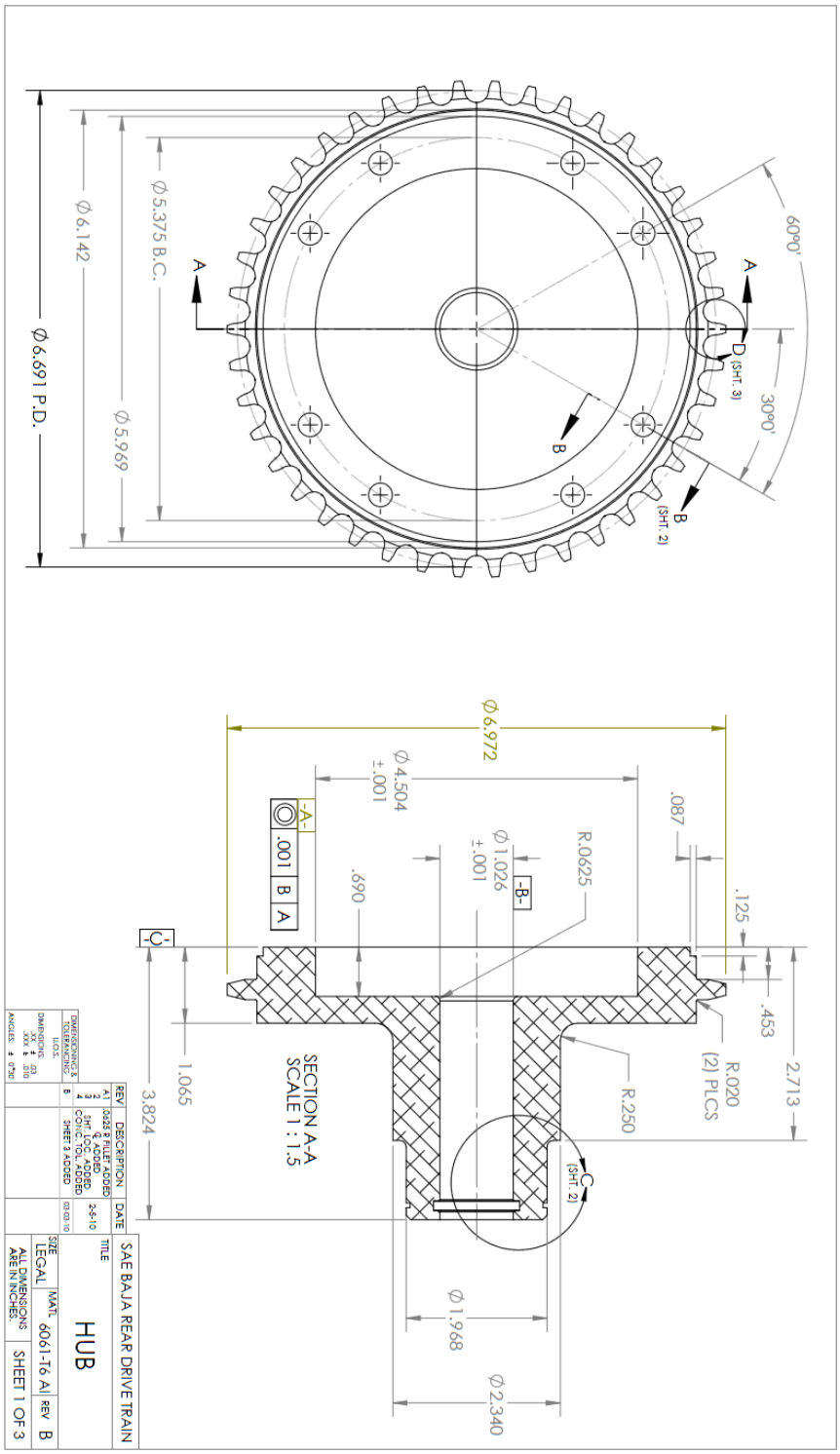

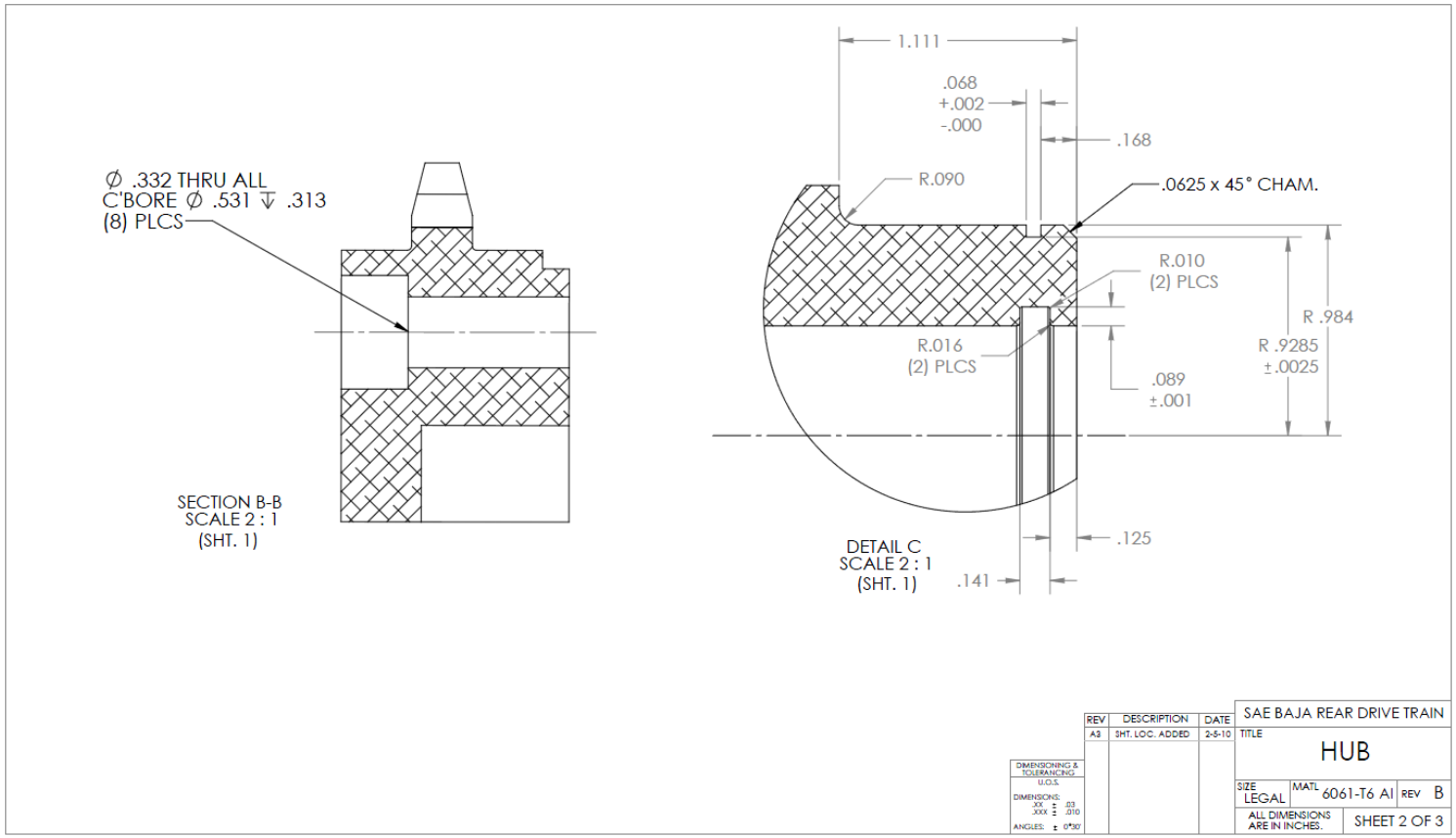

REV	DESCRIPTION	DATE
A3	SHT. LOC. ADDED	2-5-10

DIMENSIONING & TOLERANCING
U.O.S.
DIMENSIONS:
XX ± .03
XXX ± .010
ANGLES: ± 0°30'

SAE BAJA REAR DRIVE TRAIN

TITLE
HUB

SIZE LEGAL | MATL 6061-T6 Al | REV B

ALL DIMENSIONS ARE IN INCHES.

SHEET 2 OF 3

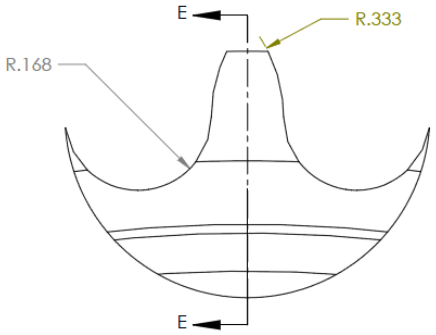

DETAIL D
SCALE 4 : 1
(SHT. 1)

SPROCKET TOOTH DIMENSIONS	
MAXIMUM DIAMETER	6.972
PITCH DIAMETER	6.691
BOTTOM DIAMETER	6.351
PITCH	.500
CHAIN #	428
NOMINAL ROLLER DIAMETER	.331
NUMBER OF TEETH	42
AVERAGE PRESSURE ANGLE	23.81°
MINIMUM PRESSURE ANGLE	15.48°
MAXIMUM HUB DIAMETER	6.142

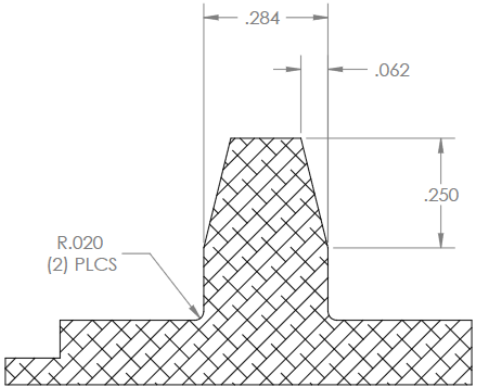

SECTION E-E
SCALE 4 : 1

REV	DESCRIPTION	DATE
B	SHEET ADDED	03-02-10

DIMENSIONING & TOLERANCING
U.O.S.
DIMENSIONS:
.XX ± .03
.XXX ± .010
ANGLES: ± 0°30'

SAE BAJA REAR DRIVE TRAIN

TITLE
HUB

SIZE LEGAL | MATL 6061-T6 Al | REV B

ALL DIMENSIONS ARE IN INCHES. | SHEET 3 OF 3

Appendix O: Internal Bearing Mount

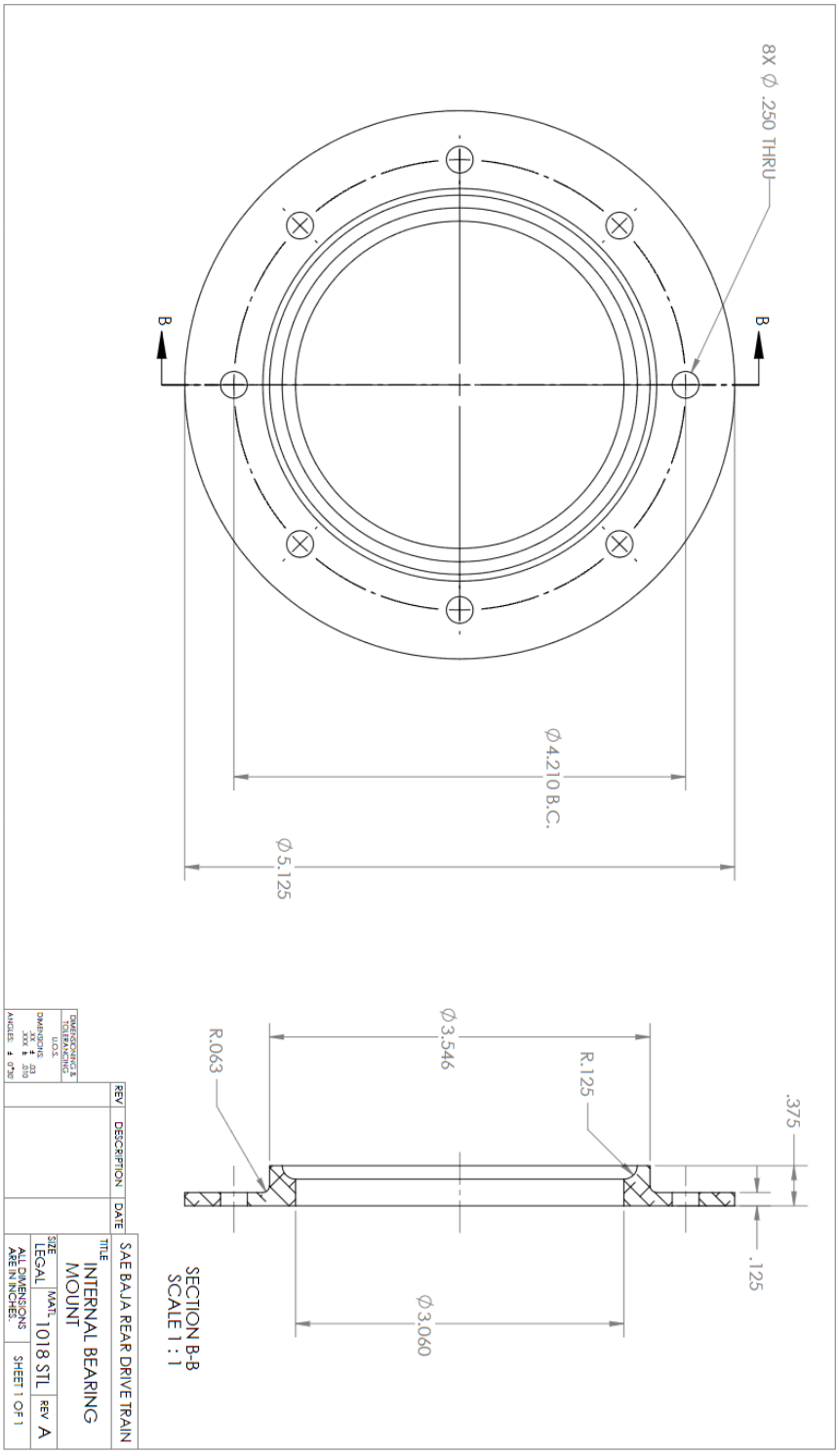

Appendix P: External Bearing Mount

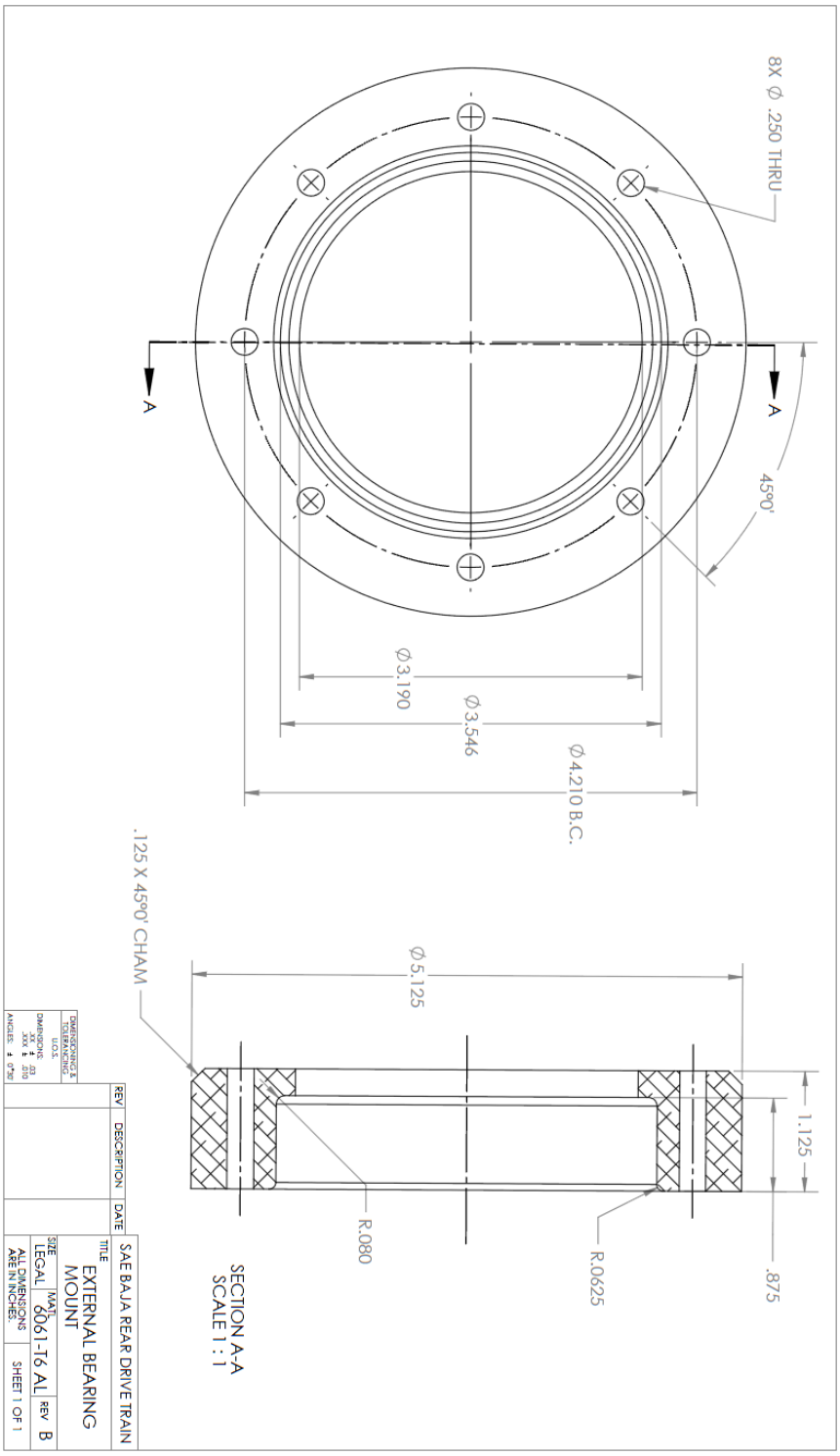

Appendix Q: Bearing Housing Assembly

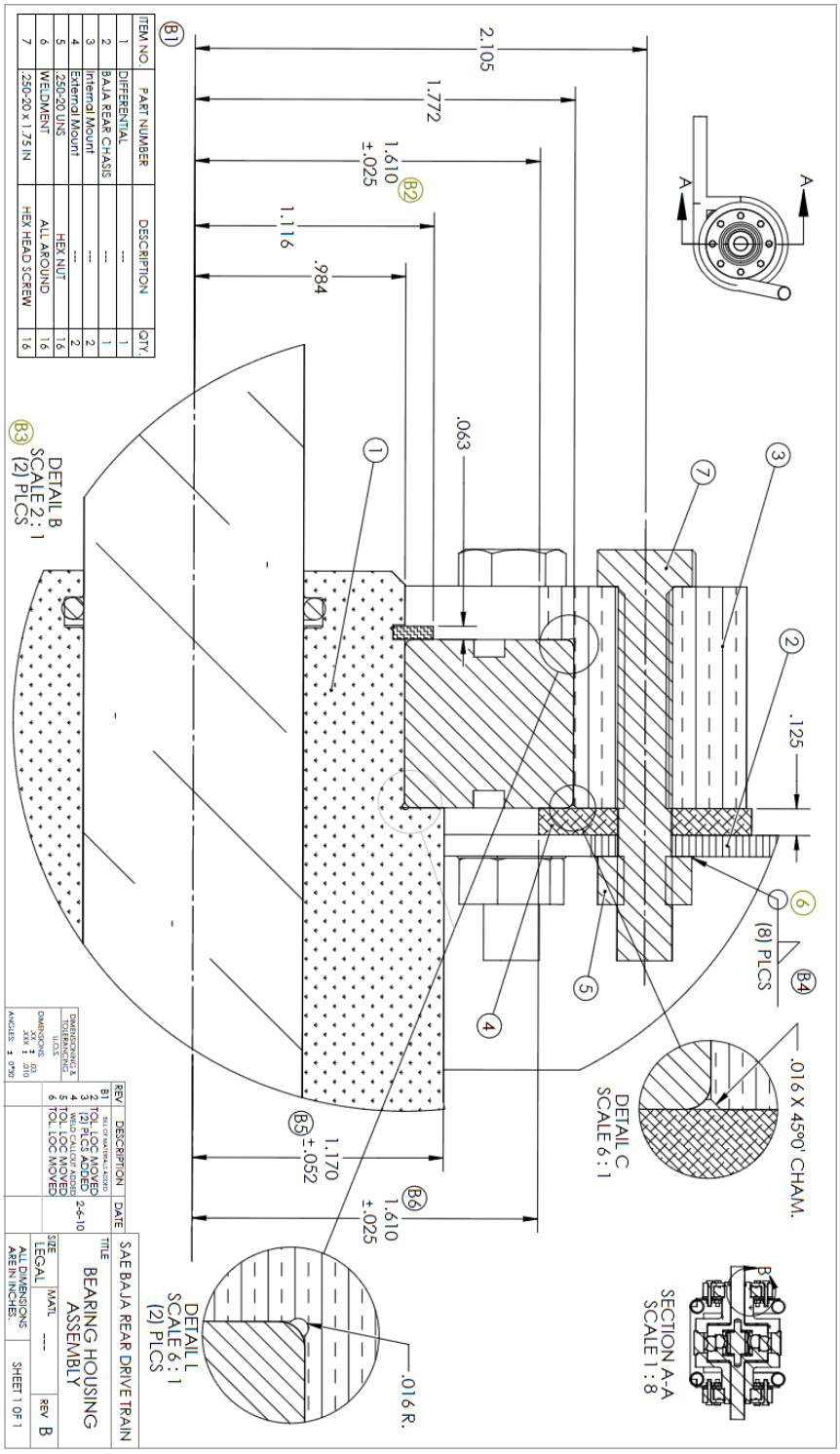

Appendix R: American National Standard Roller Chain Sprocket Flange Thickness and Tooth Section Profile Dimension

Table 6. American National Standard Roller Chain Sprocket Flange Thickness and Tooth Section Profile Dimension *ANSI/ASME B29.1M-1993 (R1999)*

Flange chamfer may be either as in Section "A" or Section "B" or anything in between.

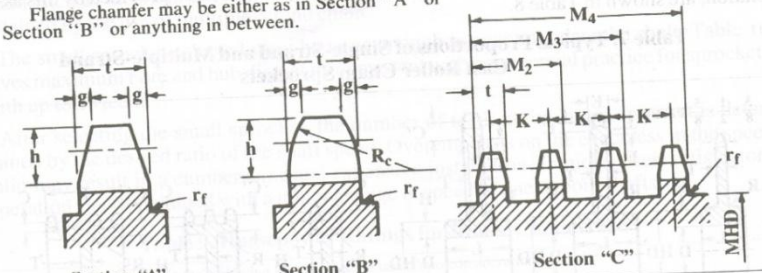

Sprocket Flange Thickness

Std. Chain No.	Width of Chain, W	Maximum Sprocket Flange Thickness, t			Minus Tolerance on t		Tolerance on M		Max. Variation of t on Each Flange	
		Single	Double & Triple	Quad. & Over	Commercial	Precision	Commercial Plus or Minus	Precision Minus Only	Commercial	Precision
25	0.125	0.110	0.106	0.096	0.021	0.007	0.007	0.007	0.021	0.004
35	0.188	0.169	0.163	0.150	0.027	0.008	0.008	0.008	0.027	0.004
41	0.250	0.226	…	…	0.032	0.009	…	…	0.032	0.004
40	0.312	0.284	0.275	0.256	0.035	0.009	0.009	0.009	0.035	0.004
50	0.375	0.343	0.332	0.310	0.036	0.010	0.010	0.010	0.036	0.005
60	0.500	0.459	0.444	0.418	0.036	0.011	0.011	0.011	0.036	0.006
80	0.625	0.575	0.556	0.526	0.040	0.012	0.012	0.012	0.040	0.006
100	0.750	0.0692	0.669	0.633	0.046	0.014	0.014	0.014	0.046	0.007
120	1.000	0.924	0.894	0.848	0.057	0.016	0.016	0.016	0.057	0.008
140	1.000	0.924	0.894	0.848	0.057	0.016	0.016	0.016	0.057	0.008
160	1.250	1.156	1.119	1.063	0.062	0.018	0.018	0.018	0.062	0.009
180	1.406	1.302	1.259	1.198	0.068	0.020	0.020	0.020	0.068	0.010
200	1.500	1.389	1.344	1.278	0.072	0.021	0.021	0.021	0.072	0.010
240	1.875	1.738	1.682	1.602	0.087	0.025	0.025	0.025	0.087	0.012

Sprocket Tooth Section Profile Dimensions

Std. Chain No.	Chain Pitch P	Depth of Chamfer h	Width of Chamfer g	Minimum Radius R_c	Transverse Pitch K	
					Standard Series	Heavy Series
25	0.250	0.125	0.031	0.265	0.252	…
35	0.375	0.188	0.047	0.398	0.399	…
41	0.500	0.250	0.062	0.531	…	…
40	0.500	0.250	0.062	0.531	0.566	…
50	0.625	0.312	0.078	0.664	0.713	…
60	0.750	0.375	0.094	0.796	0.897	1.028
80	1.000	0.500	0.125	1.062	1.153	1.283
100	1.250	0.625	0.156	1.327	1.408	1.539
120	1.500	0.750	0.188	1.593	1.789	1.924
140	1.750	0.875	0.219	1.858	1.924	2.055
160	2.000	1.000	0.250	2.124	2.305	2.437
180	2.250	1.125	0.281	2.392	2.592	2.723
200	2.500	1.250	0.312	2.654	2.817	3.083
240	3.000	1.500	0.375	3.187	3.458	3.985

All dimensions are in inches. r_f max = 0.04 P for max. hub diameter.

*This dimension was added in 1984 as a desirable goal for the future. It should in no way obsolete existing tools or sprockets. The whole depth WD is found from the formula: $WD = \frac{1}{2}D_r + P[0.3 - \frac{1}{2}\tan(90 \text{ deg} \div N_a)]$, where N_a is the intermediate number of teeth for the topping hob. For teeth range 5, $N_a = 5$; 6, 6; 7–8, 7.47; 9–11, 9.9; 12–17, 14.07; 18–34, 23.54; 35 and over, 56.

Figure 14: Machinery's Handbook (pg 2459)

Appendix S: Typical Proportions of Roller Chain Sprockets

Table 8. Typical Proportions of Roller Chain Bar-steel Sprockets

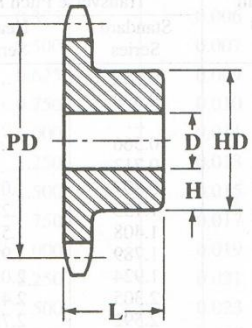

$H = Z + D/6 + 0.01\,PD$

For PD up to 2 inches, $Z = 0.125$ inch; for 2–4 inches, $Z = 0.187$ inch; for 4–6 inches, 0.25 inch; and for over 6 inches, 0.375 inch.

Hub length $L = 3.3\,H$, normally, with a minimum of $2.6H$.

Hub diameter $HD = D + 2H$, but not more than the maximum hub diameter MHD given by the formula:

$$MHD = P\left(\cot\frac{180^\circ}{N} - 1\right) - 0.030$$

where: P = Chain pitch, in inches

N = Number of sprocket teeth

Figure 15: Machinery's Handbook (pg 2460)

Appendix T: ANSI Sprocket Tooth Form For Roller Chain

Table 11. ANSI Sprocket Tooth Form for Roller Chain *ANSI/ASME B29.1M-1993*

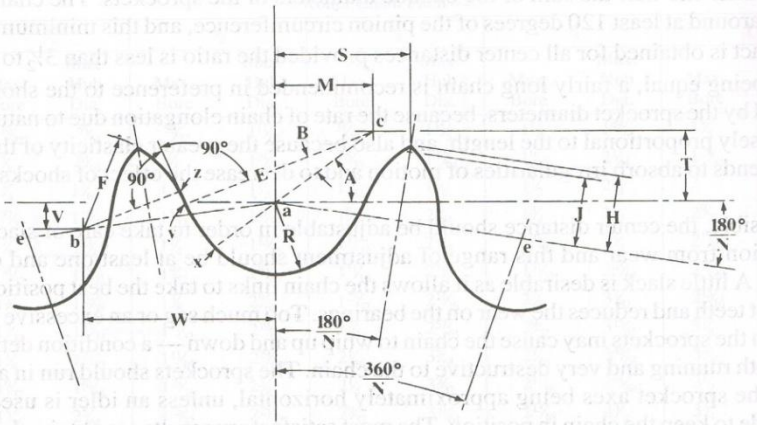

Seating Curve Data—Inches

P	D_r	Min. R	Min. D_s	D_s Tol.[a]	P	D_r	Min. R	Min. D_s	D_s Tol.[a]
0.250	0.130	0.0670	0.134	0.0055	1.250	0.750	0.3785	0.757	0.0070
0.375	0.200	0.1020	0.204	0.0055	1.500	0.875	0.4410	0.882	0.0075
0.500	0.306	0.1585	0.317	0.0060	1.750	1.000	0.5040	1.008	0.0080
0.500	0.312	0.1585	0.317	0.0060	2.000	1.125	0.5670	1.134	0.0085
0.625	0.400	0.2025	0.405	0.0060	2.250	1.406	0.7080	1.416	0.0090
0.750	0.469	0.2370	0.474	0.0065	2.500	1.562	0.7870	1.573	0.0095
1.000	0.625	0.3155	0.631	0.0070	3.000	1.875	0.9435	1.887	0.0105

[a] Plus tolerance only.

P = pitch (ae)

N = number of teeth D_r = nominal roller diameter

D_s = seating curve diameter = $1.005\,D_r + 0.003$ (in inches)

$R = \frac{1}{2} D_s$ (D_s has only plus tolerance)

$A = 35° + (60° \div N)$ $B = 18° - (56° \div N)$ $ac = 0.8\,D_r$

$M = 0.8\,D_r \cos(35° + (60° \div N))$

$T = 0.8\,D_r \sin(35° + (60° \div N))$

$E = 1.3025\,D_r + 0.0015$ (in inches)

Chord $xy = (2.605\,D_r + 0.003) \sin(9° - (28° \div N))$ (in inches)

$yz = D_r [1.4 \sin(17° - (64° \div N)) - 0.8 \sin(18° - (56° \div N))]$

Length of a line between a and $b = 1.4\,D_r$

$W = 1.4\,D_r \cos(180° \div N)$; $V = 1.4\,D_r \sin(180° \div N)$

$F = D_r [0.8 \cos(18° - (56° \div N)) + 1.4 \cos(17° - (64° \div N)) - 1.3025] - 0.0015$ inch

$H = \sqrt{F^2 - (1.4 D_r - 0.5P)^2}$

$S = 0.5\,P \cos(180° \div N) + H \sin(180° \div N)$

Approximate O.D. of sprocket when J is $0.3\,P = P\,[0.6 + \cot(180° \div N)]$

O.D. of sprocket when tooth is pointed $+ P \cot(180° \div N) + \cos(180° \div N)\,(D_s - D_r) + 2H$

Pressure angle for new chain = $xab = 35° - (120° \div N)$

Minimum pressure angle = $xab - B = 17° - (64° \div N)$;

Average pressure angle = $26° - (92° \div N)$

Figure 16: Machinery's Handbook (pg 2468)

Appendix U: Fastening MathCAD and Wrench Torque Table

$d := .250$ Bolt Diameter

$b := 3.014$

$m := 3.096$

$K := .2$ Torque Coefficient

$C_{load} := 3341$ Clamp Load

$A_t := .0318$ Tensile Stress Area

$S_p := C_{load} \cdot 1.25$ $S_p = 4.176 \times 10^3$

$F_i := .75 \cdot A_t \cdot S_p$ $F_i = 99.604$

$T_{wrench} := 10^{b+m \cdot \log(d)}$ $T_{wrench} = 14.126$ ft-lbs

$14.126 ft \cdot lb = 169.512 in \cdot lb$

$228 lb \cdot ft = 2.736 \times 10^3 \cdot lb \cdot in$

Wrench Torque $T = 10^{b+m \log d}$ for Steel Bolts, Studs, and Cap Screws (*see notes*)

Fastener Grade(s)	Bolt Diameter *d* (in.)	*m*	*b*
SAE 2, ASTM A307	¼ to 3	2.940	2.533
SAE 3	¼ to 3	3.060	2.775
ASTM A-449, A-354-BB, SAE 5	¼ to 3	2.965	2.759
ASTM A-325[a]	½ to 1½	2.922	2.893
ASTM A-354-BC	¼ to ⅝	3.046	2.837
SAE 6, SAE 7	¼ to 3	3.095	2.948
SAE 8	¼ to 3	3.095	2.983
ASTM A-354-BD, ASTM A490[a]	⅜ to 1¾	3.092	3.057
Socket Head Cap Screws	¼ to 3	3.096	3.014

Figure 17: Machinery's Handbook (pg 1429)

Appendix V: Sprocket Dimension MathCAD

Single-Strand Sprocket Dimensions

Ref: Machinery's Handbook 28th Ed. pg. 2451-2472
·ANSI/ASME B29.1M-1993 pg. 2459 and 2468

Given:

$P := .5in$ Pitch

$N_t := 42$ Number of Teeth

$D_r := .335in$ Nominal Roller Diameter (Chain # 428)

$D_s := 1.005 \cdot D_r + .003in$ $D_s = 0.3397 \cdot in$ Seating Curve Diameter

---

$R := \frac{D_s}{2}$ $R = 0.1698 \cdot in$

$A := 35deg + \left(\frac{60deg}{N_t}\right)$ $A = 0.6358$

$B := 18deg - \left(\frac{56deg}{N_t}\right)$ $B = 0.2909$

$ac := .8 \cdot D_r$ $ac = 0.268 \cdot in$

$M := .08 \cdot D_r \cdot \cos\left[35deg + \left(\frac{60deg}{N_t}\right)\right]$ $M = 0.0216 \cdot in$

$T := .08 \cdot D_r \cdot \sin\left[35deg + \left(\frac{60deg}{N_t}\right)\right]$ $T = 0.0159 \cdot in$

$E := 1.3025 \cdot D_r + .0015in$ $E = 0.4378 \cdot in$

$xy := \left(2.605 \cdot D_r + .003in\right) \cdot \sin\left[9deg - \left(\frac{28deg}{N_t}\right)\right]$ $xy = 0.1269 \cdot in$

$yz := D_r \cdot \left[1.4 \cdot \sin\left[17deg - \left(\frac{64deg}{N_t}\right)\right] - .8 \cdot \sin\left[18deg - \left(\frac{56deg}{N_t}\right)\right]\right]$ $yz = 0.0483 \cdot in$

$ab := 1.4 D_r$ $ab = 0.469 \cdot in$

$W := 1.4 \cdot D_r \cdot \cos\left(\frac{180deg}{N_t}\right)$ $W = 0.4677 \cdot in$

$V := 1.4 \cdot D_r \cdot \sin\left(\frac{180deg}{N_t}\right)$ $V = 0.035 \cdot in$

$F := D_r \cdot \left[.8 \cdot \cos\left[18deg - \left(\frac{56deg}{N_t}\right)\right] + 1.4 \cdot \cos\left[17deg - \left(\frac{64deg}{N_t}\right)\right] - 1.3025\right] - .0015in$ $F = 0.2709 \cdot in$

$H := \sqrt{F^2 - \left(1.4 \cdot D_r - .5 \cdot P\right)^2}$ $H = 0.1595 \cdot in$

$$S := .5 \cdot P \cdot \cos\left(\frac{180deg}{N_t}\right) + H \cdot \sin\left(\frac{180deg}{N_t}\right) \qquad S = 0.2612 \cdot in$$

$$OD_f := P \cdot \left[0.6 + \left(\frac{1}{\tan\left(\frac{180deg}{N_t}\right)}\right)\right] \qquad OD_f = 6.972 \cdot in \quad \text{Flat Top Outside Diameter}$$

$$OD_p := P \cdot \left(\frac{1}{\tan\left(\frac{180deg}{N_t}\right)}\right) + \cos\left(\frac{180deg}{N_t}\right) \cdot \left(D_s - D_r\right) + 2 \cdot H$$

$$OD_p = 6.9956\,in \quad \text{Pointed Outside Diameter}$$

$$OD_p - OD_f = 0.0236\,in \qquad \text{Outside Diameter Difference}$$

$$PD := \frac{P}{\sin\left(\frac{180deg}{N_t}\right)} \qquad PD = 6.6907 \cdot in \quad \text{Pitch Diameter}$$

$$BD := PD - 2 \cdot R \qquad BD = 6.3511 \cdot in \quad \text{Bottom Diameter}$$

$$APA := 26 - \frac{92}{N_t} \qquad APA = 23.8095 \qquad \text{Average Pressure Angle (Deg)}$$

$$MPA := 17 - \left(\frac{64}{N_t}\right) \qquad MPA = 15.4762 \qquad \text{Minimum Pressure Angle (Deg)}$$

$$MHD := P \cdot \left(\frac{1}{\tan\left(\frac{180deg}{N_t}\right)} - 1\right) - .030in \qquad MHD = 6.142 \cdot in \quad \text{Maximum Hub Diameter}$$

$$r_f := .04 \cdot P \qquad r_f = 0.02\,in \qquad \text{Maximum Hub Radius}$$

Appendix W: Stock Dimensions

{Quote Number: 361975}

Internal bearing Mount: $35 X 2

Steel: 1018

Quantity: 2

D = 5.25 in L = 4.3 in

(5.155 X 1.037 in)

External bearing Mount: $52 X 2

Aluminum: 6061 T6

Quantity: 2

D = 5.25 in L = 4.3 in

(5.155 X 1.037 in)

Pilot Pin: $12

High Grade steel: 1141

D = 1.1245 in L = 3.4 in

(1.1242 X 3.131in)

Pilot Bushing: $

Brass

Quantity: 1

L = 6 X 6 X 0.125 in

(2.185 X 0.125 in)

Bushing: $

Brass

Quantity: 2

L = 6 X 6 X 0.125 in

(4.469 X 0.125 in)

Cam

Quantity: 2

Steel: 1018

D = 4.625 in L = 7 in

(Part dimensions: 4.5 X 5.4 in)

Hub

Quantity: 1

Aluminum: 7075-T6

D = 6.25 in L = 4.8 in

(6.25 X 3.795 in)

Sprocket Hub

Quantity: 1

Aluminum: 6061 T6

D = 7 in L = 4.8 in

(~6.96 X 3.795 in)

Carrier

Quantity: 1

Steel: 1018

D = 6.5 in L = 2 in

(6.5 X 1.75 in)

Bearings:

Timken 366 – 362

Quantity: 2

d – Bore 1.9685 in

D - Outer Diameter 3.5433 in

T - Width 0.787 in

Appendix X: Free Body Diagrams

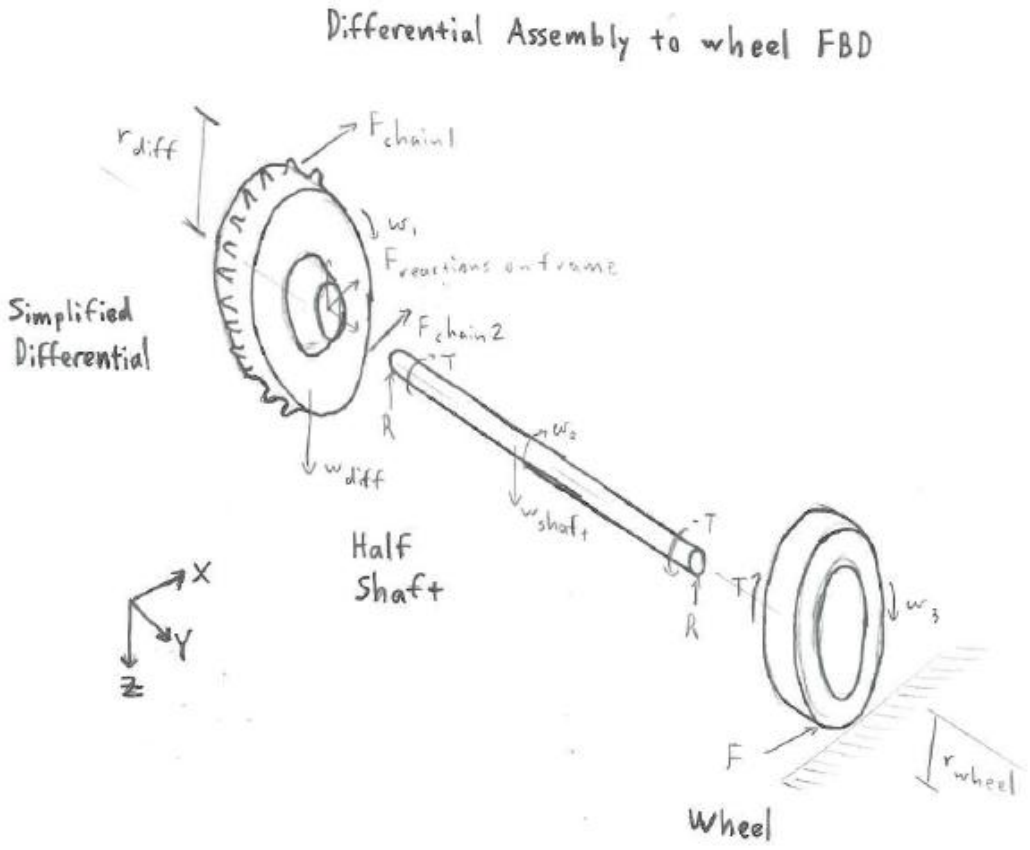

Frictional Forces Within the Differential

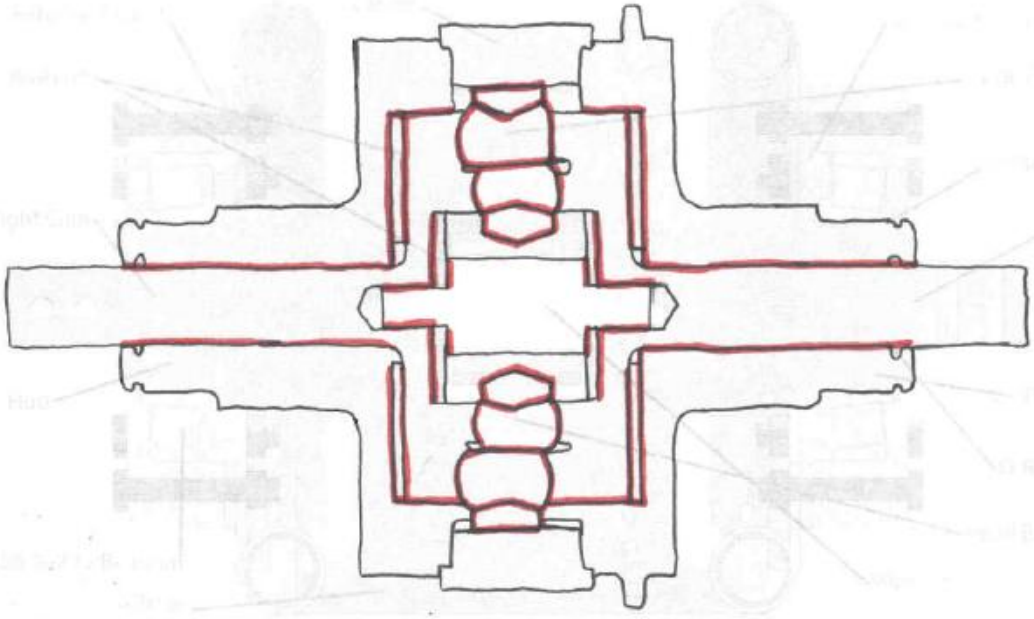

Frictional Forces at Bearings